DEVELOPMENT OF A RACING STRATEGY FOR A SOLAR CAR

A THESIS SUBMITTED TO
THE GRADUATE SCHOOL OF NATURAL AND APPLIED SCIENCES
OF
MIDDLE EAST TECHNICAL UNIVERSITY

BY

ETHEM ERSÖZ

IN PARTIAL FULFILLMENT OF THE REQUIREMENTS
FOR
THE DEGREE OF MASTER OF SCIENCE
IN
MECHANICAL ENGINEERING

SEPTEMBER 2006

Approval of the Graduate School of Natural and Applied Sciences

_____

Prof. Dr. Canan Özgen
Director

I certify that this thesis satisfies all the requirements as a thesis for the degree of Master of Science

_____

Prof. Dr. Kemal İder
Head of Department

This is to certify that we have read this thesis and that in our opinion it is fully adequate, in scope and quality, as a thesis for the degree of Master of Science

_____

Asst. Prof. Dr. İlker Tarı
Supervisor

Examining Committee Members

Prof. Dr. Y. Samim Ünlüsoy	(METU, ME)	_____
Asst. Prof. Dr. İlker Tarı	(METU, ME)	_____
Asst. Prof. Dr. Cüneyt Sert	(METU, ME)	_____
Asst. Prof. Dr. Derek Baker	(METU, ME)	_____
Prof. Dr. A. Erman Tekkaya	(Atılım Ü., ME)	_____

I hereby declare that all information in this document has been obtained and presented in accordance with academic rules and ethical conduct. I also declare that, as required by these rules and conduct, I have fully cited and referenced all material and results that are not original to this work.

Name, Last name : Ethem ERSÖZ

Signature :

ABSTRACT

DEVELOPMENT OF A RACING STRATEGY
FOR A SOLAR CAR

Ersöz, Ethem
M. S., Department of Mechanical Engineering
Supervisor : Asst. Prof. Dr. İlker Tarı

December 2006, 93 pages

The aerodynamical design of a solar race car is presented together with the racing strategy. Dealing with the design and the racing strategy simultaneously offers the advantage of having improvements on both, using the results of each other. Besides these, as a prerequisite of the design, the decision on number of the wheels is discussed. If the three wheel configuration is selected, the requirements for having the desired performance while eliminating the risk of tipping over are inspected.

In the aerodynamics analyses, the software packages Gambit and Fluent are utilized. Using the results of the CFD simulations, aerodynamical shape of the body is analyzed to determine weak points of the design, causing early boundary layer detachment and higher drag. The drag coefficient of the body is also obtained from CFD runs at various speeds. It was determined that the selected NACA profile performs well, under racing speeds but the canopy design is open to improvement.

The racing strategy is analyzed using the race track information together with the

design of the solar car. A program was created to determine the position, velocity, acceleration and power consumption versus time. Also the lap time and total energy consumption can be obtained and these are vital data while determining their sensitivity to mass or to resistances. By the help of this program, the experience gained by completing laps on the circuit can be partially gained without actual laps.

Keywords: Solar Energy, Race, Vehicle, Car, Strategy

ÖZ

GÜNEŞ ENERJİLİ YARIŞ ARABASI İÇİN
YARIŞ STRATEJİSİ GELİŞTİRME

Ersöz, Ethem
Yüksek Lisans, Makine Mühendisliği Bölümü
Tez Yöneticisi : Yard. Doç. Dr. İlker Tarı

Aralık 2006, 93 sayfa

Güneş enerjili bir yarış aracının aerodinamik tasarımı yarış stratejisi ile birlikte ele alınmıştır. Aerodinamik tasarımı yarış stratejisi ile birlikte ele almanın getirdiği bir avantaj, her iki çalışmanın sonuçlarının, diğerini geliştirmek üzere kullanılarak tekrarlanması sonucu tasarımın daha ileriye gidebilmesidir. Bunların yanında tasarımın bir ön koşulu olarak aracın kaç tekerlekli olacağı, eğer üç tekerlekli olursa istenen çevikliği sağlarken, devrilmemesi için gereken şartlar incelenmiştir.

Aracın aerodinamik analizlerinde Gambit ve Fluent yazılımları kullanılmıştır. Analizlerden elde edilen sonuçlar, tasarımın akışın ayrılmasına ve aerodinamik direncin artmasına neden olan zayıflıklarını görmeyi sağlamıştır. Sonuçlardan, aynı zamanda aerodinamik direnç katsayısı da elde edilmiştir. Yarış hızlarında gövde için seçilen NACA profilinin hedeflenen performansı gösterdiği, kanopinin ise geliştirilebileceği görülmüştür.

Yarış stratejisi, pist geometrisi ve eğimler verisi ve aracın tasarım özellikleri birlikte dikkate alınarak oluşturulmuştur. Aracın pist üzerinde zamana bağlı

konumunu, hızını, ivmesini, birim zamanda harcadığı enerjiyi hesaplayan bir program oluşturulmuştur. Aynı zamanda, tur süresi ve toplam enerji tüketimi gibi yarış stratejisi belirlemede kullanılan hayati değerler, kütle ve dirençlerdeki değişikliklerin bunlar üzerine etkileri de bu programı kullanarak elde edilebilir. Bu sayede araç piste çıkıp gerçek turlar atmadan, atıldığında kazanılacak deneyim kısmen elde edilebilmektedir.

Anahtar Kelimeler: Güneş Enerjili, Yarış, Araç, Araba, Strateji

To My Family

ACKNOWLEDGEMENTS

The author wishes to express his deepest gratitude to his supervisor Asst. Prof. Dr. İlker TARI for his guidance, advice, criticism, encouragements and insight throughout the university education and the graduate studies. The author has always felt confident by feeling him watching from a distance and sharing his valuable experiences, whenever needed.

The author would also like to thank to all members of the Team Hasat for their hard work and to main financial supporter Atilim University, especially to Prof. Dr. A. Erman TEKKAYA for his belief in his students which made this expensive project possible.

TABLE OF CONTENTS

LIST OF TABLES

LIST OF FIGURES

NOMENCLATURE

A_{cs}	Frontal drag area of the car [m^2]
C_d	Total drag coefficient [ ]
CG	Center of gravity
R_E	Distance between the Earth the Sun [m]
a	Distance of center of gravity from the front axle [m]
a_{corr}	Effective distance of center of gravity from the front axle corrected for the slope [m]
b	Distance of center of gravity from the rear axle [m]
b_{corr}	Effective distance of center of gravity from the rear axle corrected for the slope [m]
e	Distance from center of gravity to the tipping axes the axles on top view [m]
f	Distance from center of gravity to the tipping axes on top view [m]
h	Height of the center of gravity [m]
t_f	Front track width [m]
t_r	Rear track width [m]
v	Velocity [m/s]
w	Weight of the vehicle + 75 kg [kg]
wb	Wheelbase [m]
α	Angle between the tipping axis and the symmetry axis [º]
θ	Angle of the slope [º]
μ	Static coefficient of friction between the tire and the road material [ ]
ρ	Roll angle [º]

ABBREVIATIONS

CFD	Computational Fluid Dynamics
FIA	Fédération Internationale de l'Automobile
NACA	National Advisory Committee for Aeronautics

CHAPTER 1

INTRODUCTION

This thesis work is a step in creating a solar car which utilizes solar energy efficiently, in body design and control strategy. The solar car is designed and produced by the Hasat team in cooperation with Atılım Üniversitesi to participate in the first solar car race in Turkey. The thesis presents the problems in body design and racing strategy encountered during the preparation for the race and also develops an effective approach to solve the most important minority of the problems.

The problems encountered during the design stage are in wide range of importance and solution difficulty. Initially, the problems need to be determined. Next the priorities to the solutions of each problem are assigned. The general approach of the team to problem solving is presented in Table 1.1.

Table 1.1 Problem types and decision making on solution priority

Problem types	Primary	Secondary
Easy to solve	A) solve first	B) grade and compare
Hard to solve	C) grade and compare	D) be aware

The importance of the solution of a problem can be compared with the others by calculating the gain in lap time, if it is a problem related to the performance. It may be related to safety; in this case, the importance is rather hard to assign. It may affect the reliability of the car or the costs in time and money. Generally, a problem is related to more than one of these three categories (performance, safety and

reliability) with some tradeoffs in between.

Under these conditions, the team has sometimes chosen to leave solutions of some problems as a room for improvement in the future versions of the car. The problematic situation for the team is to encounter a problem in the race that is not even considered before.

After all, the ultimate goal in the race is to achieve the shortest time for the race with limited budget in design and construction and using limited energy in the race. The ultimate goal in this thesis is to provide an approach in directing the limited sources to the most favorable points.

1.1 Formula-G

Formula-G is the annual solar car race organization in Turkey. The race was first organized in 2005, by Tübitak (Turkish Scientific and Technical Research Council). It took place on the same track nine days after the first Formula 1 race in Istanbul. This organization differs from most of the solar car races in the world by the track it is held on. This makes this race very demanding both in the design stage and during the race. In the second year, the race was organized in two stages and both of them were on less demanding race tracks.

1.2 Other Solar Car Races in the World

Solar car racing is not a new type of challenge. Australian World Solar Challenge is the first one organized in 1987. It starts from Darwin, in the north of Australia, and ends in Adelaide in the south of Australia. The distance in between is 3000 km. Since then, the cars evolved very fast. This can be seen by comparing the

average speeds:

The first World Solar Challenge was staged in 1987, with a field of 23 fantastic cars led by the GM Sunraycer which completed the trip with an average speed of 67 km/h. [1]

The last race held in 2005 was won by Nuna 3 with an average speed of 103 km/h [1].

The American Solar Challenge is a race starting at Austin, Texas and ending in Calgary, Alberta, on about 2500 mile length course which changes from race to race [2]

The following is a list of the solar races in the world [3]:

- American Solar Challenge (USA)
- Formula Sun Grand Prix (USA)
- Winston Solar Challenge (USA)
- Dell-Winston School Solar Car Challenge (USA)
- Australian World Solar Challenge (Australia)
- Suzuka (Japan)
- WSTM 2003 (Malaysia)
- World Solar-Car Rallye (Japan)
- 2006 World Solar Rally (Taiwan)
- Phaeton 2004 (Greece)
- SunRace (Australia)

Most of them are long road races as opposed to Formula-G which takes place on a Formula 1 track. As a result, Formula-G requires a different race strategy then other solar car races.

1.3 Formula-G Race Track

In 2005, the race track was Istanbulpark Formula 1 race track. The geometry and slopes of the track is given in Figure 1.1.

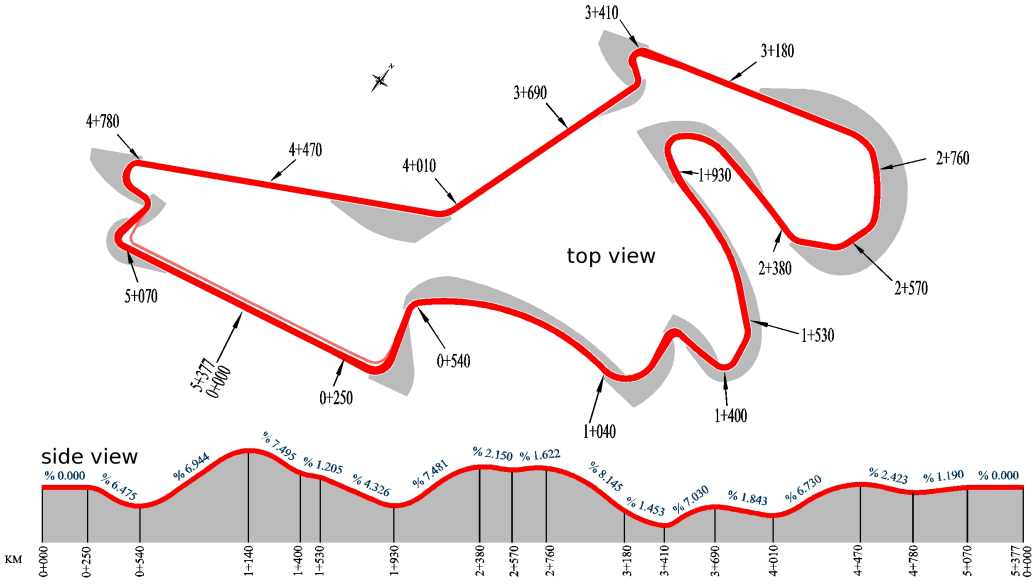

Figure 1.1 Turkish Formula 1 racing circuit İstanbulpark

The side view in Fig. 1.1 has the wrong 1+140 marking, whereas the top view denotes the same point as 1+040. The original figure is given here while using 1040 m in the calculations. This can be checked by noting that the elevation difference must be zero between the start and the ending point on a closed circuit.

The first race that the team participated in was held in İstanbulpark, the Formula 1

track of Turkey. Therefore the design is strongly affected from the fact that, the car will not travel on a long and straight route as in the most solar races in the world. In this type of races weight affects the performance more, whereas aerodynamic resistance affects the performance less. What makes Formula-G more difficult is the characteristics or the shape of the circuit. The shape of the circuit is interesting in different aspects. The 8^{th} curve starting at 2+380 with 4 apexes in the same direction is very famous for being demanding among the Formula 1 drivers. Also, the sharpest corners are just at the end of long straights where high speed is reached. These can be seen by just looking at the map of the circuit in Fig. 1.1. When the top view and the side view in Fig. 1.1 are considered together, the real problem for solar vehicles becomes clearer. The two steepest and long downhill parts are followed by curves with the smallest radii of curvature (curves at 1+930 and 3+420). Therefore all the kinetic energy gained while going down the slope is wasted by heating the discs of the brakes unless the motor has regenerative braking ability.

The first curve, turning left, is at the end of the 630 m long start/finish straight. The cars approaching at this curve need to slow down, because this is a sharp curve tilting outward. In addition, just before the curve, a downhill gradient of 6.475% starts. This requires braking harder, whereas the energy getting lost is required for the next uphill gradient with 34.8 m of altitude change in 500 m. The ability to take the curve as fast as possible plays an important role in saving energy and time here. A car with lower CG (Center of Gravity) and high lateral acceleration ability is strictly required. The second curve was not problematic in the first race but, when faster cars take the first curve faster, with the help of the downhill gradient in between, it will be another critical point to analyze. The third curve is not critical, being at the top of the longest uphill gradient and having a large radius of curvature. The fourth and the fifth curves are again a problem of a trade off between cornering safety and energy saving. The sixth curve at 1+530 can be disregarded, having a large radius of curvature, but the seventh curve just at the

bottom on the side view at 1930 m from the start, is the same problematic type of curve. The eighth curve, the nightmare of Formula 1 drivers is one of the easiest ones for Formula-G drivers. It is at a high altitude and the speed is already low there and also the radius of curvature is very large compared to the other curves. Then, there is the nightmare of the Formula-G drivers. It is just after the steepest downhill gradient on the track (8.145%). The fact that it is downhill is not helpful because the ninth curve at the end is the sharpest one on the track. The change in altitude, between 2760 m and 3410 m is 37.5 m. In frictionless conditions, when an object at rest is released from the top, it reaches the end with 97 km/h. In fact, it is out of the design range of the electric motor. The speed limit was around 80 km/h. In the actual case, the speed reaches 70 to 75 km typically. The following (9^{th}) curve must be taken as fast as possible just as in the case of the first and the seventh curves, but this time more severely, to climb the 7.030% gradient of 280 m long. The braking applied here slows the car from around 70 km/h (20 m/s) to below 40 km/h (10 m/s). The amount of energy loss can be roughly calculated for a 330 kg of mass as 14 Wh. It will be estimated in Section 5.2 that the energy available for one lap is around 225 Wh. Therefore, more than 6% of total energy is lost just at this point. Twelfth, thirteenth and fourteenth curves form a chicane. After gaining some speed at the end of a downhill gradient of 290 m, following the ideal line makes it possible to have some advantage over the opponents skipping the importance of it.

In fact, except the 630 m of start/finish straight there is no level road. Everywhere else is either uphill or downhill gradient mostly varying between 5% and 8%. This is steeper than the slopes encountered in European highways, at which the maximum gradient is 4%. Therefore, considering the need for frequent accelerations and decelerations, importance of the weight of the car increases and the aerodynamic drag coefficient becomes relatively less important while compared to the other solar car races. Aerodynamics of the car is still important because it is still one of the main reasons of energy loss.

1.4 Formula-G Race Rules

Race rules were announced to be the same as the ones applied by the FIA (Federation Internationale de l'Automobile) [4]. Therefore, some of the design parameters were obtained from the rules. The dimensions of the car were limited with 5 m of length and 1.8 m of width. Number of wheels had to be between 3 and 6. The car had to start moving upwards on a slope with 18% gradient. The weight of the car had to be between 150 kg and 300 kg without the driver. There had to be a roll bar to protect the driver if the car turns over. The driver had to wear a 5 point racing harness. But since this was the first time this race was being held, some of the requirements were not inspected. Therefore the application of the rules can be said to be not strict.

1.5 Motivating Aerodynamics and Importance of Racing Strategy

The importance of having a strategy can be seen in the results of two years (Tables 1.2 and 1.3). The winner of the 2005 race has the longest best time, disregarding the uncompetitive 9^{th} car. The car with the best time in 2005 could complete only 3 laps. The reason for this was lack of energy. In the second year, as can be seen in Table 1.3, the best times are more realistic. The aim was to complete 30 laps in 90 minutes. This required a mean lap time of 3 minutes. This time, there are no teams completing very fast laps and experiencing lack of energy. The energy is distributed to the laps more evenly. This shows that having a strategy is definitely helpful. After this point, improving or optimizing the strategy is required.

The aim in the strategy chapter of this thesis (Chapter 5) is to demonstrate the approach to the problem; some values for the car or its performance may not be exact because some of them are not measured. This leads to finding a

demonstrative result, which is not the actual one. On the other hand the method used is still ready to give the correct result when the input is corrected. The lap time calculation is repeated several times with various inputs, to see the effects of change of parameters while keeping the lap time or energy consumption constant. Additionally, two alternative improvements having the same cost can be compared. One improvement such as a 10% decrease in air drag coefficient can be compared with 5% of decrease in weight. If the team has to choose only one of these improvements due to some limitations, then the improvement in the lap time in each case must be known, to be able to compare objectively.

1.6 Race Results

The race route was changed in 2006 to bypass the long uphill gradient starting at 540 m in Fig 1.1. As a result of this, one lap distance became 2.2 km. This change from 5.4 km/lap to 2.2 km/lap must be kept in mind while comparing the results of two years. However, the only effect on the lap time is not the length of the circuit, the circuit is modified by bypassing the steep gradients with level shortcuts. Therefore the characteristics were totally changed.

The results of 2005 races are given in Table 1.2 and the results of 2006 races are given in Table 1.3.

Table 1.2 Formula-G 2005 Race Results

Position	Team	Completed Laps	Shortest Lap Time	Average Speed
1	ORT	8	9:53.349	22.803
2	**Hasat**	**7**	**8:39.952**	**22.563**
3	YUGAT	6	7:24.238	22.580
4	Saguar	6	6:48.392	18.482
5	ODTÜ	5	7:55.266	23.672
6	Hitit Güneşi	5	9:17.919	14.729
7	Solaris	4	8:45.649	27.885
8	YTU-GESK	3	6:32.696	13.490
9	Ceryan	2	24:09.605	16.410
10	Türk Mekatronik	1	-.---	15.311
11	Gazi	0	-.---	-
12	ITU-GAE	0	-.---	-
13	GYTE & Sabancı	0	-.---	-
14	TaTo	0	-.---	-
15	ACI	0	-.---	-
16	Isparta	0	-.---	-

Table 1.3 Formula-G 2006 Race Results

Position	Team	Completed Laps	Shortest Lap Time	Average Speed
1	ARIBA - 1	30	2:42.872	42.772
2	ARIBA - 2	28	2:53.937	40.188
3	BARRACUDA	25	3:11.131	35.138
4	ODTU - TEK	25	2:52.159	34.816
5	TIMSAH	25	3:08.391	34.465
6	**HASAT 1B**	**24**	**3:16.289**	**33.429**
7	N.R.G.	23	3:39.566	32.875
8	SOULAR CAR - 1	23	3:16.545	32.150
9	OSCAR	20	3:50.776	28.367
10	ERKE	20	3:27.229	27.086
11	THEIA	18	3:45.846	25.724
12	SUNRISE	13	4:28.242	19.187
13	Dr. G	13	4:34.642	18.488
14	TYEK - G	13	4:01.668	16.191
15	MARTI	11	3:19.832	16.639
16	SCU - 1	9	3:18.356	36.460
17	EGEFE	7	2:55.529	12.839
18	BSG	3	3:46.916	20.733

1.7 The Ideal Design Procedure

The reported work in this thesis represents the procedure of design and construction in the way that is realized. The real procedure was different from the ideal one. To be able to see the difference, the ideal procedure is given in Figure 1.2.

In the teamwork, the flow chart was followed without any loops. Each stage was done once and the last two analysis blocks were completed with rough estimations due to lack of experimental data.

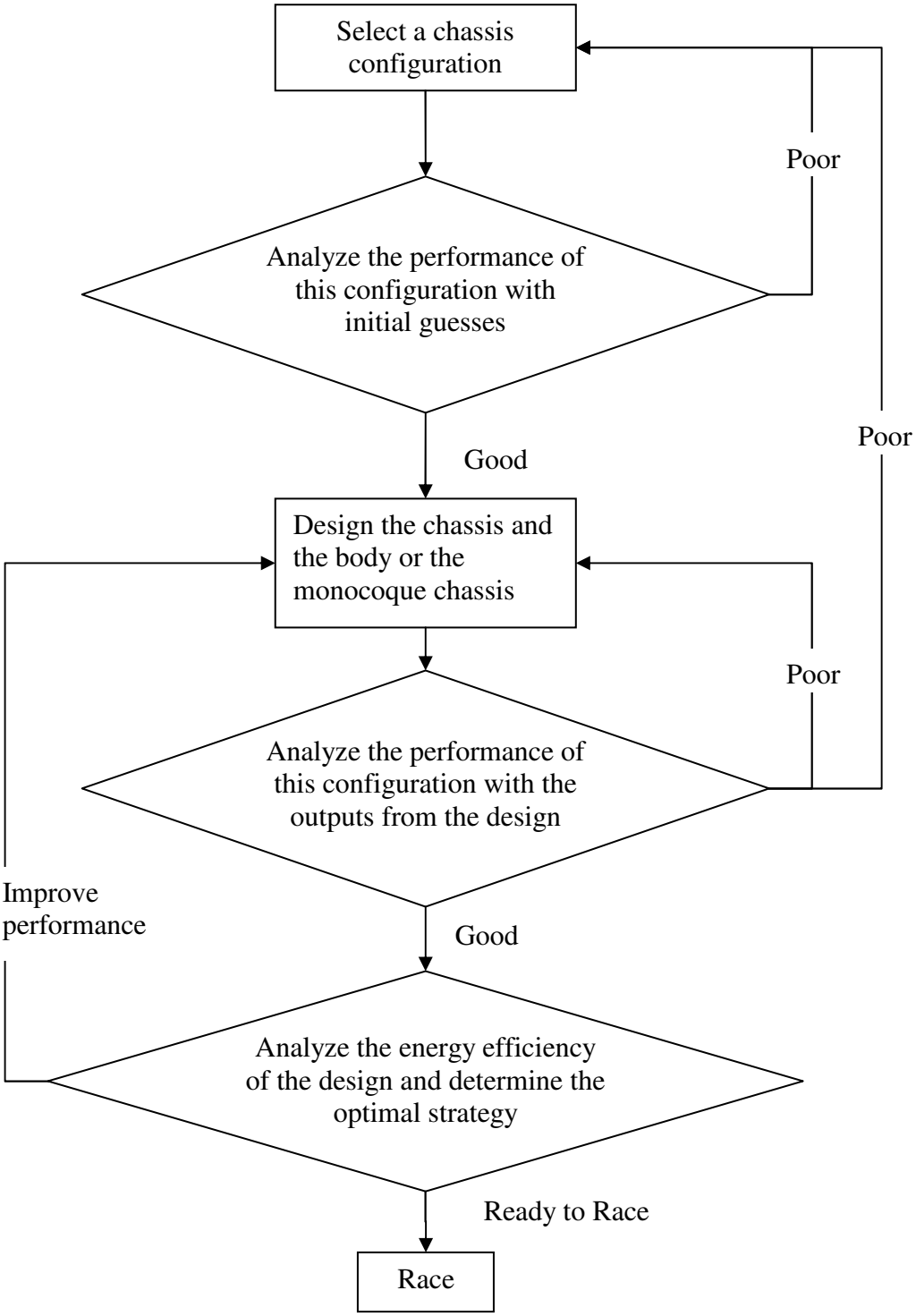

Figure 1.2 The ideal design procedure

1.8 Comparison of Hasat 1A with Aurora Solar Car

The Aurora team has been in the solar races from the beginning. The team finished the World Solar Challenge 2nd in 1987 and has been successfully racing from then on [5]. The team history starts with a race ending in 2nd position and continues with a race ending in 6th position just as in the Hasat's case. The team has been improving their cars continuously. The reason for selecting this team as an example is given below as explained in the team's website:

In the last 24 months, Aurora has set 8 new world records, including the longest solar car journey (13,054 km around Australia in 24 days), and has broken world records set by previous champions Honda (Japan), Biel (Switzerland) and Queens (Canada). Spurred on through competition, Aurora is one of two teams to compete in all seven World Solar Challenge events, has consistently been the best Australian entrant, the only Australian winner (1999), and second place getter in 1987, 2001 and 2003. Aurora currently (November 2004) holds 9 world records. [5]

Therefore, the comparison chart presented in Table 1.4 must be considered as a comparison of the initial design of an inexperienced team with the upper limit in this category.

Table 1.4 Comparison of Hasat with Aurora Solar Car

	Aurora The 2005 Car	**Hasat** Hasat 1A (2005)
Dimensions [mm]		
Length	4628	4998
Width	2000	1760
Height	946	1056
Wheelbase	1680	2500
Track	1600 (rear)	1600 (front)
Chassis		
Weight (w/o driver) [kg]	165	240
Frame	carbon fiber, circular cross section Single front wheel Two rear wheels	aluminum, circular cross section Two front wheels Single rear wheel
Wheels		
Size	16”	16”
Front	motor integrated	steel motorcycle wheel
Rear	GH Craft carbon fiber	motor mounted steel motorcycle wheel
Tires	Low rolling resistance	slick racing tires
Brakes	Hydraulic on all wheels Regenerative in front	Hydraulic on all wheels
Aerodynamics		
C_d	0.19 (Wind Tunnel)	~0.34 (CFD)
Frontal Area [m^2]	0.75	1.13
Solar Cells		
Efficiency	24-26%	13%
Weight [kg/m^2]	<1	~1.2
Array Power [W]	1900	800
Motor		
Weight [kg]	15	29
Peak Power [kW]	6	14.4 limited to 3
Continuous Power [kW]	1.8	8 limited to 3
Efficiency	98%	>95%
Batteries		
Type	Lithium Polymer	Lead acid
Weight [kg]	30 kg	30 kg
Capacity [kWh]	4	1

Comparing the cars, it can be seen that Hasat is 75 kg heavier than Aurora. The weight difference is mainly because of the monocoque carbon fiber structure of Aurora. Secondly, carbon fiber wheels and integrating a lighter motor into the front wheel make the difference. Aurora also has a very slim profile and this reduces frontal cross sectional area, which improves the car aerodynamically. Since the power output of the panels is limited with 800 W, the body was still kept large and this allowed cheaper panels to be used in Hasat. The motor of Hasat is very heavy. The requested motor from the supplier could not be acquired in time and the motor described in the table was used in the race. It is used by limiting its power because of some reliability problems with the driver. The motor was also expected to have the regenerative braking ability, but after a failure just before the race, this feature was disabled. Comparing the efficiencies of the motors, it seems that they are both very efficient but, these values are given for a prescribed range of speed and power. The electric motor of Hasat was limited to 20% of its maximum power; therefore its efficiency may be lower in this range.

Another important difference between the cars is the battery technologies. Hasat has the Lead-Acid batteries, whereas Aurora is equipped with Lithium Polymer batteries. If the same capacity of batteries of Aurora was packed by Lead-Acid type batteries, the pack would weigh 120 kg.

Besides these, the low rolling resistance tires, ideal steering because of the single front wheel, very low drag coefficient and cross sectional area allow the car to demand less power while cruising at the same speed with Hasat.

1.9 Comparison of Hasat with Arıba of İstanbul Technical University

Arıba was probably the most advanced solar car in the organization in 2005. However the race ended very early for it in the first year. The team had not given up for the next year. They had brought the first Arıba, labeling it Arıba I and a new one Arıba II. Both were at least 60 kg lighter than Hasat 1B. Arıba II was probably more advanced in the sense that it is built with more experience but in the races Arıba I was the leader for most of the time. This can be because of the difference in driving skills but on the other hand there is the probability that after their first year experience the team may have chosen to be more conservative to increase reliability.

The advantages of Arıba I and Arıba II over Hasat 1B are not just their lightness. The higher efficiency cells requiring half of the area of Hasat's allow a smaller car. This leads to smaller cross sectional area which decreases pressure drag. Also the total area of friction is less and that reduces viscous drag.

The communication between Arıba and the pit crew allowed flow of some data from the car and in turn the team could adjust the performance of the car, possibly with a similar approach to the one presented in this thesis.

The special tires manufactured for solar racing cars with half the rolling resistance is another advantage over standard motorcycle tires of Hasat.

CHAPTER 2

BACKGROUND

2.1 The Need for Alternative Energy Vehicle Technologies

Before making a solar car, the ease or the cost of construction and the usability of the solar car must be checked for feasibility before spending money and time on design and construction. It must be shown that this effort is to find a way out, not for satisfaction of curiosity. Therefore some facts about world energy use patterns must be investigated. In this chapter, this feasibility check is done.

2.1.1 Predictions about Oil Reserves Depletion

The average power consumption per person in the U. S. was 13.2 kW in the year 2001 [6]. This energy is supplied easily, therefore cheaply, because it is extracted from the vast storage of fossil fuels. But, this storage is finite. Therefore one can extrapolate the oil consumption data, taking some effects into account and foresee some date for the depletion of the reserves [7]. The important point to concentrate on is the date when the cost of oil reaches the cost of the alternatives for the same work capacity, i.e. the cost of heating or traveling using alternative energy sources. After that, oil prices will saturate because of the availability of alternatives. From there on despite the increase in production cost, the price can not increase following the same trend. When extraction of oil increases up to a point such that it is no longer profitable because of the fixed or decreasing prices of the alternatives, it will no longer be feasible. Therefore the alternative energy vehicles or hybrid cars are likely to gain considerable market share starting from the date the prices

come close to each other.

2.1.2 Effect of Burning Fossil Fuels on the Environment

Another consequence of burning fossil fuels in today's high rates is the greenhouse effect which may lead to dramatic changes in climates all over the world. In fact some of its impacts are observable like sudden and excessive rainfall in some parts of the world, thickening/widening desert band and notable change in total mass of ice at the poles but, this is not new [8]. The environmental conditions must also be checked before making long term predictions. If there will be lack of drinking water in 20 years, which leads to wars, which leads to dramatic changes in the world's population, then it is hard to guess the trend of oil usage of 30 years from now.

2.2 Justification of the Need for Solar Energy on the Road

The reasons stated above yield the need for alternative energy resources. Since energy storage is still a problem, the next solution is continuously recharging a rather small storage. This is possible with solar energy with the advantage of no special refueling locations or no continuous connection to mains as electric trains require.

With all these in mind, it is important to know, to what extent, solar energy is reliable. Let the distance from the Sun to Earth be R_E. Then the solar irradiation on a sphere with a radius R_E, with Sun at the center is 1537 W/m^2. This comes down to around 1000 W/m^2 on the Earth surface, for a horizontal plate, but only around the equator because of absorption and reflection back to the space.

Using the meteorological data for Istanbul, Turkey, [9] the daily solar energy available can be calculated for an average day. Afterwards, how many liters of gasoline gives this energy when burnt in an internal combustion engine can be calculated as an answer to the question, to what extent the solar energy can be thought of as a power source.

Using the data in hand, the daily solar energy available is around 7000 Wh/m^2 in August and at least 6000 Wh/m^2 in September. On a vehicle which is built according to FIA (Federation Internationale de l'Automobile) regulations, there is 9 m^2 of area of which typically 7 m^2 out of it can be covered with solar panels because of the need for a canopy for example. Knowing these, the daily available energy for August becomes 49000 Wh and for September at least 42000 Wh. But these are obtained when the panel area normal follows the sun.

Typically a vehicle will have fixed horizontal panels. So the solar power times direction cosine must be integrated over time with direction cosine as a function of time. When this is done, a typical value for August becomes 5500 Wh/m^2 and for September it becomes 4500 Wh/m^2. These lead to totals of 38500 Wh and 31500 Wh consecutively.

Assuming panel efficiency of 20%, while 39% of efficiency is available but expensive [10], the energy available to charge the batteries becomes 7700 Wh (27720 kJ) every day. Today cell efficiencies of 39% are being reported [10]. Of course, these high efficiencies are obtained in the laboratories, where the cells are kept at 25°C. But the technology advancement has not saturated yet.

Taking the coefficients used in the Shell Eco Marathon into account, the net calorific value of reference fuel Shell Formula Super 95 is 32010 kJ/lt, as stated in Shell Eco-marathon Rules & Regulations.

The definition of net calorific value is as follows:

Net calorific value can be defined as quantity of heat liberated by the complete combustion of a unit of fuel when the water produced is assumed to remain as a vapor and the heat is not recovered; also known as lower heating value. [11]

Assuming that, the efficiency is 30% in an internal combustion engine. This means that 9600 kJ of work can be extracted from 1 lt of gasoline. When compared to 27720 kJ of energy which can be extracted from 2.9 lt everyday (including weekends) corresponds to 87 lt for a typical August in Istanbul. This seems to contribute a considerable amount. Maybe for some people it will supply all their energy needs.

When the data for last 4 years of Istanbul, Turkey, where the race will be held, is inspected, it is seen that solar irradiation on a horizontal area changes between 760-840 W/m^2 at noon. This is very close to the position of the panels on the solar cars. Since the race is to start at 11:00 and end at 13:00 (in 30th August 2005), a fair mean value of 800 W/m^2 can be used to obtain the upper limit in the calculations for energy available during the race.

However, the regulations state that the power output (maximum 800 W in our case) of the solar panels will be calculated using the following formula:

power output = panel area * panel efficiency * 1000 W/m^2 of solar irradiation

The amount of solar irradiation is given as 1000 W/m^2 in the rules, whereas practically the limit for the race location is 800 W/m^2. Therefore the practical peak

panel output becomes 80% of the allowed limit which is 640 W.

2.2.1 Solar Energy as an Auxiliary Supply for the Hybrid Car of the Future

Obviously one doesn't want to rely only on solar energy to supply his needs while there are additional constraints on performance at night or uncertainties on cloudy days. To increase reliability and to delimit the daily consumption, another power supply can be utilized which can be an internal combustion engine or a fuel cell.

Another aspect of having plenty of solar vehicles, as stated in the above paragraphs, is the need for parking areas without shadow. This is impossible for most of the large city centers in the world with very dense population, but it is easy to supply in most of the world where population density is low and latitudes less than 45º. This part of the problem must be dealt with a multi disciplinary approach with city planning professionals.

2.3 Solar Vehicle as a Race Car

While designing a vehicle as a race car, every part must be designed keeping the ultimate goal of completing the race in shortest possible time. Therefore the design depends strongly on the rules, regulations and limitations on the car and the driver. There is one important difference between the conventional motor sports races and solar racing. That is the limitation on the total power available; the power output of the panels is limited. The limiting value may change depending on the panel efficiency, available area or the solar energy available at that location, but there is always a limit. Moreover, in a solar race, the battery capacities are kept low on purpose, to show what the solar power can do. The batteries are intended to supply the short term, high power demands.

Keeping all these in mind, the race actually starts with the design procedure. Design factors i. e. weight, shape, material, reliability and safety factors affect the result. All these must be as efficient as possible. The thesis work presented here represents a part of the work to design an efficient race car.

2.4 Previous Work on Solar Car Racing Strategy

Before talking about design and the optimal race strategy of a solar car, a basic description on how a solar car works must be given. Various approaches on the subject are explained in the following paragraphs:

The paper, titled “Optimal Design of a Hybrid Electric Car with Solar Cells” [12] starts with a similar approach as in this thesis and states that “Some recent studies of the UK government report that about 71% of UK users reaches their office by car, and 46% of them have trips shorter than 20 min., mostly with only one person on board.”. This requirement can be satisfied with solar cars with zero fuel cost. This shows that using simpler and lighter vehicles can both respect the environment and decrease the total transportation cost. In this paper also a sensitivity analysis was carried out, to study the effects of design variables on vehicle performance, weight and cost.

The paper, titled “Solar Eclipse: The Failure of a Promising Technology” [13] was published in the year 2000. It states that the technology of solar cars has saturated before the existence of a product that meets the needs of the targeted market. Actually the technology of solar panels has not saturated yet and there has been some improvement from then on [12]. The availability of cheaper and more efficient panels may require reconsideration of the subject.

The paper, titled “Design and Construction of a Solar Electric Commuter Car” [14] attempts to convert a Volkswagen Beetle, with a fiber glass body kit, into a solar car. The solar panels have 500 W of peak power output and the car weighs 720 kg. It does not look promising when compared to 165 kg weight and 1900 W of peak power output of Aurora Solar Car, but it claims that safety is more important and this car would fulfill the daily transportation requirements.

The paper, titled “Solar Car Cruising Strategy and its Supporting System” [15] approaches the problem with a very similar approach. It is concentrated on the application of the strategy but the reasoning is not explained in detail. In this thesis, the reasoning is given and a similar strategy is preferred for the simulations.

CHAPTER 3

CHASSIS CONFIGURATION

The chassis of a car is the structure that all the other components are loaded on. It is also expected to provide a safe cage to the driver and the passengers if exist.

In a solar race car, these are also expected and in addition a roll bar with a certain load carrying capacity is required [4] (the "2004 - Technical Regulations for Electro-Solar and Alternative Energies Vehicles" handbook). If the total weight of the car and the driver (taken as 75 kg) is called w, the roll bar needs to withstand 1.5 w, 5.5 w and 7.5 w in lateral, front/rear and vertical directions respectively. Hasat 1A is equipped with a roll bar conforming to the rules. A few demonstrative figures from the analysis done by the team designer Orçun Yıldırım are given in the appendix.

Besides these safety properties, the chassis is the part determining the dynamics and the driving characteristics of the car. In essence, the driving characteristics can be thought of as the chassis being driven with every other part loaded as a dead weight. Except the air drag, which changes with the shape of the body, nothing changes with the change of other elements as long as the weight and the location of center of gravity are conserved.

In this chapter, the most suitable configuration for the car is to be determined. The chassis can be designed for strength afterwards, because the points of action and magnitudes of the forces are determined by the configuration and the position of center of gravity.

3.1 Chassis Design

3.1.1 Configuration Selection

While designing the chassis, one should decide on the number of wheels, first. There are two practical choices: a three-wheeled or a four-wheeled configuration. For the desired simplicity of design, which includes less number of movable parts, less number of total parts, less weight and cost, the three-wheeled configuration is advantageous. In case it cannot be achieved, the 4 wheel design is the second choice. A simple comparison is given in Table 3.1.

Table 3.1 Advantages of configuration alternatives

3 wheels	**4 wheels**
The desired choice Advantages: ● less number of movable parts ● less weight ● less cost ● one-wheel symmetric traction ● ideal steering	In case the other configuration can not be designed to perform safely in terms of tipping over tendency during cornering. Advantage: ● almost no risk of tipping over

The problem with three-wheeled configurations is the risk of instability. When the center of gravity with fixed height moves towards the single wheel, the car will tend to tip over. Conversely, when it moves towards the axle with 2 wheels, the tipping over or rolling tendency decreases. Therefore, from the cornering ability point of view, the center of gravity that is close to double wheeled axle is preferred.

On the other hand, with simplicity and efficiency in mind, it is better to drive the

car with a single motor. Otherwise, a mechanical differential with a certain mechanical efficiency or an electrical differential between two motors must be used which reduces reliability and efficiency and increases cost and weight.

With one wheel hub motor in hand there is one more decision to make: whether symmetry is required or not. Symmetry simplifies the design of numerous parts. Since this is the first vehicle to be designed by the team, due to lack of experience, it is not desirable to encounter any unpredictable driving characteristics due to an asymmetric structure.

At this stage the configuration is with three-wheels and the motor is on the single wheel. The only decision left here is where the single wheel will be situated. Two more considerations affect the remaining decision: ideal steering requirement for higher efficiency and the requirement to climb 18% gradient from rest. A short MATLAB™ program is written for determining the limiting distances of center of gravity from both axles. To be able to find the most suitable configuration, all possible ones needs to be listed. This list is given in Table 3.2.

Table 3.2 List of possible chassis characteristics

3 wheels								**4 wheels**							
Symmetric				Asymmetric				Symmetric				Asymmetric			
1 motor		2 motors		1 motor		2 motors		1 motor		2 motors		1 motor		2 motors	
F	R	F	R	F	R	N	N	X	X	F	R	F	R	N	N
F: motor in front axle, R: motor at rear axle, N: not discussed, X: impossible with wheel hub motors															

The advantageous selection can be followed from Table 3.2 as 3-wheeled, symmetric, single motor, as described in the previous paragraphs. The last decision left is whether the single wheel will be in front or rear. If the single wheel is situated in front, then ideal steering is also satisfied automatically. The only disadvantage, but an important one, is the weight transfer due to gradient. The

acceptable zone (for the location of center of gravity) between stability and grading ability requirements is larger for rear wheel driven case. Since this is an initial trial and the height of center of gravity can not be known precisely beforehand, to be on the safe side, giving up the advantages of ideal steering, the design is chosen as 3 wheeled, symmetric, single motor at the rear axle. (3S1R)

Among the other choices presented in Table 3.2, the 3-wheeled, symmetric, single motor at the front axle 3S1F is a preferable solution if the height of center of gravity can be as low as required or the grading and cornering requirements are not so severe. The asymmetric 3A1F configuration is not a preferable one unless the steering is at the rear wheel but rear wheel steering is not considered because of stability problems.

The 3A1R configuration is another preferable one. Ideal steering is already satisfied. The stability in the corners and grading ability requirements are both satisfied better, if the center of gravity is closer to the rear axle. The only possible disadvantage of this may be the yawing moment due to eccentricity between the driven wheel and the center of gravity. However with solar cars having long wheelbase (>2.5m) and short track (~1.4m) (low track/wheelbase ratio) and driven in low acceleration range, this effect is negligible.

3.1.2 Load Distribution

The only predicted (uncertain) value here is the friction coefficient. In fact the real value can never be determined and there is not a constant value, because in practice it changes according to both road conditions and tire conditions, which are affected by the weather, local asphalt quality/type, thread pattern and wear percentage of the wheel and so on. Therefore an acceptable value must be used here. Still, to be on the safe side, in the MATLAB™ code (`gradeability.m`), the design is performed by taking the coefficient of friction under the tractive tire as 0.5, but to avoid tipping, a cornering lateral acceleration ability of 1g or even

slightly higher is expected from the car in `rollmodel.m` program as the tipping over limit. This makes the car start sliding before tipping in the case of a coefficient of friction of 1.

Since, in the beginning of such a construction without any available selected parts, it is hard to estimate the height of the center of gravity of the final design. To be prepared for the worst case, it is taken as 0.6 m, which is the height of the highest point on the upper body shell from the ground plane.

With the fixed height of center of gravity and friction coefficient, the limiting values for center of gravity to the axles for climbing the 18% gradient for rear wheel driven case and front wheel driven case are obtained as shown in Table 3.3.

3.1.2.1 `Gradeability.m` MATLAB™ Program

`Gradeability.m` is one of the two programs written to help on chassis configuration decisions. The inputs to this program are the geometrical parameters of the car and the friction coefficient between the tire and the asphalt. The most important output of the program is the location of the center of gravity along the vertical symmetry plane of the car with given height, to satisfy the ability to climb up the gradient of 18%. Two other outputs are the torque requirement and with given power available to the motor, the maximum speed at which the 18% gradient can be climbed. The code of the file is given in its original syntax in Table 3.3. The explanation of the code in the form of classical equations is given under the "3.2 Verification of `gradeability.m`" title.

Table 3.3 `Gradeability.m`

Inputs:	Description:
wb= 2.5;	wheelbase [m]
h= 0.6;	height of center of gravity [m]
mu= 0.5;	coefficient of friction [ ]
M= 340;	total mass of the vehicle [kg]
gr= 0.18;	gradient to climb
g= 9.81;	gravitational acceleration [m/s^2]
rw= 0.225;	wheel radius [m]
power=3000;	power [W]

Solution:	
ang=asin(gr);	angle of inclination [rad]
angle=ang*180/pi	angle of inclination [º]
%friction limited	
disp('min a and max b for rear axle driven case');	rear wheel driven case
aprimer=wb*tan(ang)/mu;	minimum effective a on that gradient [m]
bprimer=wb-aprimer;	maximum effective b on that gradient [m]
armin=aprimer-h*tan(ang)	minimum a in rear wheel driven case [m]
brmax=bprimer+h*tan(ang)	maximum b in rear wheel driven case [m]
disp('max a and min b for front axle driven case');	front wheel driven case
bprimef=wb*tan(ang)/mu;	minimum effective b on that gradient [m]
aprimef=wb-bprimef;	maximum effective a on that gradient [m]
afmax=aprimef-h*tan(ang)	minimum a in rear wheel driven case [m]
bfmin=bprimef+h*tan(ang)	maximum b in rear wheel driven case [m]
% torque limited case	torque limited case
fmotor=M*g*gr	tractive effort output of the motor-wheel assembly [N]
Tmotor=fmotor*rw	motor cutoff torque [N*m]
v1=power/fmotor	maximum speed attainable with the given power on that gradient [m/s]

3.1.2.2 `Rollmodel.m` MATLAB™ Program

`Rollmodel.m` is written to evaluate the limiting lateral acceleration value of tipping over, while cornering. The geometry of the car is the input. The first output of the program is the limiting lateral acceleration at which the car will tip over with rigid suspension. The second output is the limiting lateral acceleration with the

modified geometry because of the suspension deflection. Therefore, both the limiting acceleration and the effect of suspension deflection can be obtained. The explanation of the code in the form of classical equations is given under the "3.3 Verification of `rollmodel.m`" title.

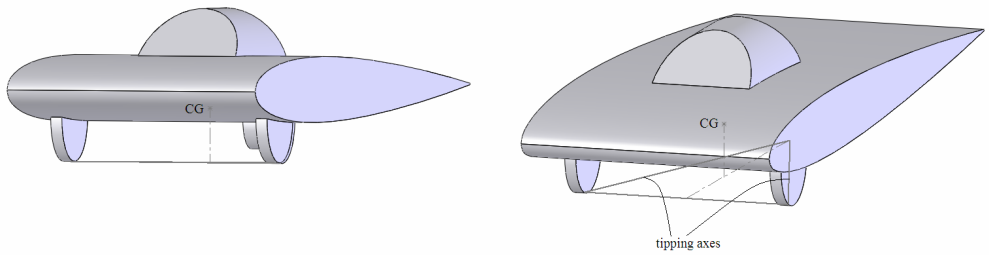

Figure 3.1 The tipping axes and the position of center of gravity
left: view along tipping axis
right: slightly tilted view showing the base of the car formed by the tipping axes

The compliance referred in the program is used instead of torsional suspension stiffness which is angular deflection per moment on the system. It is angular deflection per lateral acceleration. The relation between these quantities can be summarized as:

i. Torsional stiffness of the suspension [Nm/deg]

ii. Difference between the height of center of gravity and the height of the roll center in front view [m]

iii. Force acting on center of gravity under the action of lateral acceleration [N/g] (g: gravitational acceleration in units of m/s^2)

iv. Torque acting on the suspension under the action of lateral acceleration is the product of ii and iii leading to [Nm/g] in units.

v. Dividing iv by i gives torsional stiffness under the action of lateral

acceleration [g/deg]

vi. Reciprocal of this quantity, which can be called compliance [deg/g]

Compliance is preferred in the program because it can be reached directly from the modeling program. In case of absence of this ability, it can be calculated as explained above.

The geometry considered in the program is given in Fig. 3.2 in top view.

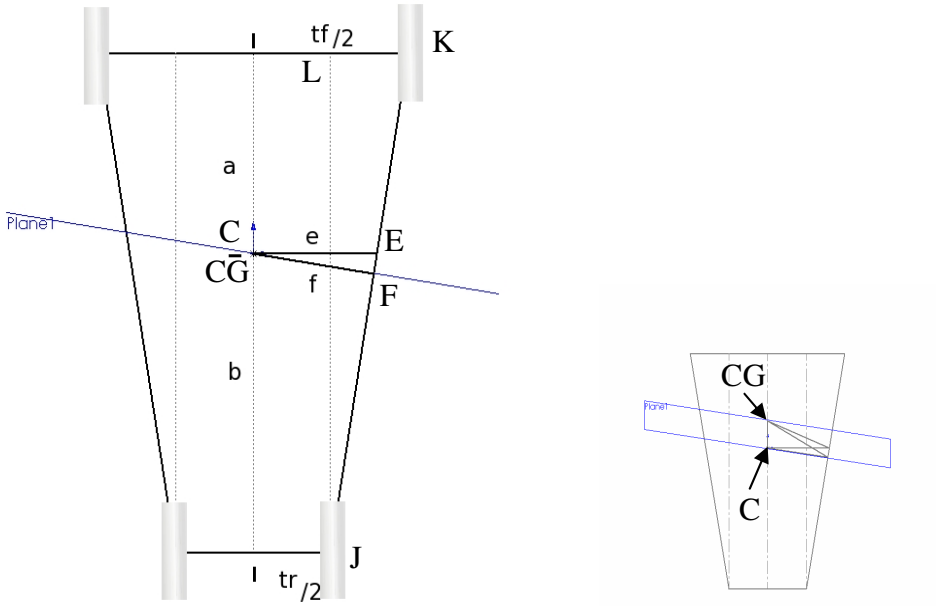

Figure 3.2 Sketch of top view of the car, with tires at the corners
The variables a, b, e, f, tf, tr are shown. Height of CG is h

The input of the `rollmodel.m` is given in Table 3.4. The equations the program used are given in Table 3.5 in the m-file syntax and the equations are given below as Eqn. 3.1 and Eqn. 3.2 for the case tr<tf.

Table 3.4 `Rollmodel.m` input

Input:	
a=2;	distance between center of gravity and the front axle along the longitudinal direction [m]
b=0.5;	distance between center of gravity and the rear axle along the longitudinal direction [m]
h=0.6;	height of center of gravity
tf=0;	front track
tr=1.6;	rear track
r=0.05 %	angular compliance under lateral acceleration [rad/g]
unit='rad/g'	
rr=r*180/pi	angular compliance based on lateral acceleration [deg/g]
unit='deg/g'	

Table 3.5 `Rollmodel.m` case tr<tf solution

Case tr<tf solution	
if tr<tf	
acc=((tr/2)+b/(b+a)*(tf-tr)/2)*cos(atan((tf-tr)/2/(a+b)))/h	Eqn. 3.1
condition='lateral acceleration for tr<tf and stiff suspension'	
correct='correction taking the roll stiffness into account'	
acceleration=(((tr/2)+b/(b+a)*(tf-tr)/2)*cos(atan((tf-tr)/2/(a+b))))*(1-sin(acc*r)))/(h*cos(acc*r))	Eqn. 3.2
end	

$$acc = \frac{1}{h} \times \left(\frac{t_r}{2} + \frac{b}{b+a} \frac{t_f - t_r}{2} \right) \times \cos\left(atan\left(\frac{t_f - t_r}{2(a+b)} \right) \right) \tag{3.1}$$

$$acceleration = \left(\frac{\frac{t_r}{2} + \frac{b}{b+a} \frac{t_f - t_r}{2} \cos\left(atan\left(\frac{t_f - t_r}{2(a+b)} \right) \right) - \sin(acc \times r)}{h \cos(acc \times r)} \right) \tag{3.2}$$

The equations the program used are given in Table 3.6 in the m-file syntax and the equations are given below as Eqn. 3.3 and Eqn. 3.4 for the case tr>tf.

Table 3.6 `Rollmodel.m` Case tr>tf solution

Case tr>tf solution if tf<tr condition='lateral acceleration for tf<tr and stiff suspension' acc=((tf/2)+a/(b+a)*(tr-tf)/2)*cos(atan((tf-tr)/2/(a+b)))/h correct='correction taking the roll stiffness into account' acceleration=(((tf/2)+a/(b+a)*(tr-tf)/2)*cos(atan((tr-tf)/2/(a+b)))- sin(acc*r))/(h*cos(acc*r)) end	Eqn. 3.3 Eqn. 3.4

$$acc = \frac{1}{h} \times \left(\frac{t_f}{2} + \frac{a}{b+a} \frac{t_r - t_f}{2} \cos\left(atan\left(\frac{t_r - t_f}{2(a+b)} \right) \right) \right) \tag{3.3}$$

$$acceleration = \left(\frac{\frac{t_f}{2} + \frac{a}{b+a} \frac{t_r - t_f}{2} \cos\left(atan\left(\frac{t_r - t_f}{2(a+b)} \right) \right) - \sin(acc \times r)}{h \cos(acc \times r)} \right) \tag{3.4}$$

3.2 Verification of `gradeability.m`

The verification can be done by following the derivation steps. Derivation of the formula for obtaining the grading ability limit of the car is given below.

Fig. 3.3 is the sketch of the vehicle in side view. The aim of `gradeability.m` is to calculate the limiting positions of CG along the symmetry axis. This gives an interval for “a” or “b”.

Considering the rear wheel driven case, the load on the rear wheel must be at least

$$\frac{a'}{a'+b'} mg = \frac{\tan(\theta)}{\mu} mg \tag{3.5}$$

to prevent slip.

$$a' + b' = a + b = wb \tag{3.6}$$

Where, wb stands for wheelbase.

Note that the a' value obtained from here is the limiting value which means smallest a' in this case. Rearranging

$$a' = wb\frac{\tan(\theta)}{\mu} \tag{3.7}$$

Converting back to horizontal position

$$a = a' - h\tan(\theta) \tag{3.8}$$

This is the minimum a value in rear wheel driven case. The maximum b value can be found as

$$b = wb - a \tag{3.9}$$

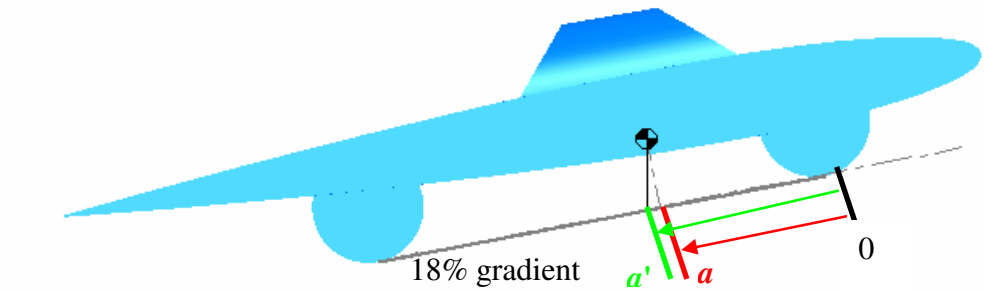

Figure 3.3 Side view of the car while climbing the 18% gradient

The output of `gradeability.m` file, in this case is:

- The minimum *a* and maximum *b* values for the rear wheel driven case
- The maximum *a* and minimum *b* values for the front wheel driven case
- The torque requirement for the motor, knowing the radius of the driven wheel
- Up to what speed this motor can provide this torque or what the maximum speed is on that gradient, given the power of the motor.

There is a trade off between lateral stability and grading ability, because moving CG close to the front axle improves lateral stability, whereas moving CG close to rear axle improves grading ability. Therefore the `rollmodel.m` and `gradeability.m` files may be used iteratively to get an acceptable solution. The search for an optimal solution is meaningless. Since the solution depends on the maximum and minimum values of coefficient of friction the solution changes depending on these. These change with the track surface type and quality and tire.

Derivation of the formula for obtaining the lateral acceleration limit of the car without tipping over is given below.

3.3 Verification of `rollmodel.m`

Fig. 3.2 is the sketch of the wheels' positions and tipping axes. There are 4 wheels in this figure because the program is able give the result for a 4 wheel configuration. The figures about the real car have 3 wheels. These figures are obtained by setting the rear track equal to zero, since there is a single wheel at rear. The wheels shown in the figure are all on the road surface. The only point out of the road surface is the point CG with height h. Since the problem is symmetric, it is enough to investigate the conditions while turning to one side only. The case considered here is taking a left curve, i.e. turning counter-clockwise when viewed from above. The aim of `rollmodel.m` is to calculate the ratio of length f to height of center of gravity at first step. This is given as *f/h* in the derivation below.

This will give the limiting lateral acceleration for the car with stiff suspension. Formulation is as follows.

Using similarity of triangles ΔJLK and ΔCEF in Fig. 3.2

$$\frac{(t_f - t_r)}{\frac{2}{a+b}} = \frac{e - \frac{t_r/2}{b}}{b} \tag{3.10}$$

From here

$$e = \frac{t_r}{2} + \frac{b\left(t_f - t_r\right)}{2\left(a+b\right)} \tag{3.11}$$

Calling the angle between e and f which is also equal to the angle between the tipping axis and the symmetry axis "α":

$$\alpha = atan\left(\frac{t_f/2 - t_r/2}{a+b}\right) \tag{3.12}$$

And finally

$$f = e\cos\left(\alpha\right) \tag{3.13}$$

Rearranging

$$f = \left(\frac{t_r}{2} + \frac{b\left(t_f - t_r\right)}{2\left(a+b\right)}\right)\cos\left(atan\left(\frac{t_f/2 - t_r/2}{a+b}\right)\right) \tag{3.14}$$

The ratio *f/h* is calculated as

$$f/h = \frac{1}{h}\left(\frac{t_r}{2} + \frac{b\left(t_f - t_r\right)}{2\left(a+b\right)}\right)\cos\left(atan\left(\frac{t_f/2 - t_r/2}{a+b}\right)\right) \tag{3.15}$$

This can be called the aspect ratio.

More precisely, taking the line of action of centripetal force acting on CG into account, the force is actually along e and it acts along f. Therefore the cos(α) term should drop in the limiting acceleration with stiff suspension case. The actual line of action is unknown since the slip angles of each tire at that speed are unknown. Therefore there is always the possibility of having the centripetal force along f, with the help of acceleration, which is the worst case. Even if the force is along e, then that term can be considered as a safety factor because it allows for some acceleration during cornering. In case of single front wheel, this term allows some deceleration which is likely to occur in practice.

When the suspension deflection is taken into consideration the tipping triangle is altered. This affects the aspect ratio depending on the suspension stiffness.

To see the effect of suspension deflection on the aspect ratio, the geometric roll center of the suspension must be determined. For the double wishbone with parallel and equal length "A" bracket configuration the roll axis is the intersection of the road surface and the longitudinal symmetry plane of the car.

To calculate the amount of roll around this axis, angular roll stiffness must be known. This can be determined with a geometrical solution if the stiffnesses of the suspension elements are known. Alternatively, the car can be loaded around the axis with a moment and the angular deflection can be measured.

Knowing the roll center and the amount of roll around that axis, the new location

of CG while cornering, at the tipping limit is obtained.

The new aspect ratio is the limiting lateral acceleration.

$$a_{corr} = \frac{f - f\sin(\rho)}{h\cos(\rho)} \tag{3.16}$$

Where a_{corr} stands for corrected limiting lateral acceleration, rearranging

$$a_{corr} = \frac{f\left(1-\sin(\rho)\right)}{h\cos(\rho)} \tag{3.17}$$

$$a_{corr} = \frac{\left(\frac{t_r}{2} + \frac{b}{b+a}\frac{t_f - t_r}{2}\right)\cos\left(atan\left(\frac{t_f - t_r}{2(a+b)}\right)\right)\left(1-\sin(\rho)\right)}{h\cos(\rho)} \tag{3.18}$$

Where, ρ is the roll angle. In Figure 3.4, it is the angle between the vertical solid line and the dotted line from the center of the circle to the new CG location.

As can be seen from the figure,

- The higher the roll center, the less the CG is displaced. (Assuming that the roll center is below CG.)
- The higher the torsional stiffness of the suspension, the less the CG is displaced.

Therefore high roll stiffness is desirable and if for some other reasons suspension needs to be soft, then a suitable anti-roll bar can be added to improve the performance against tipping.

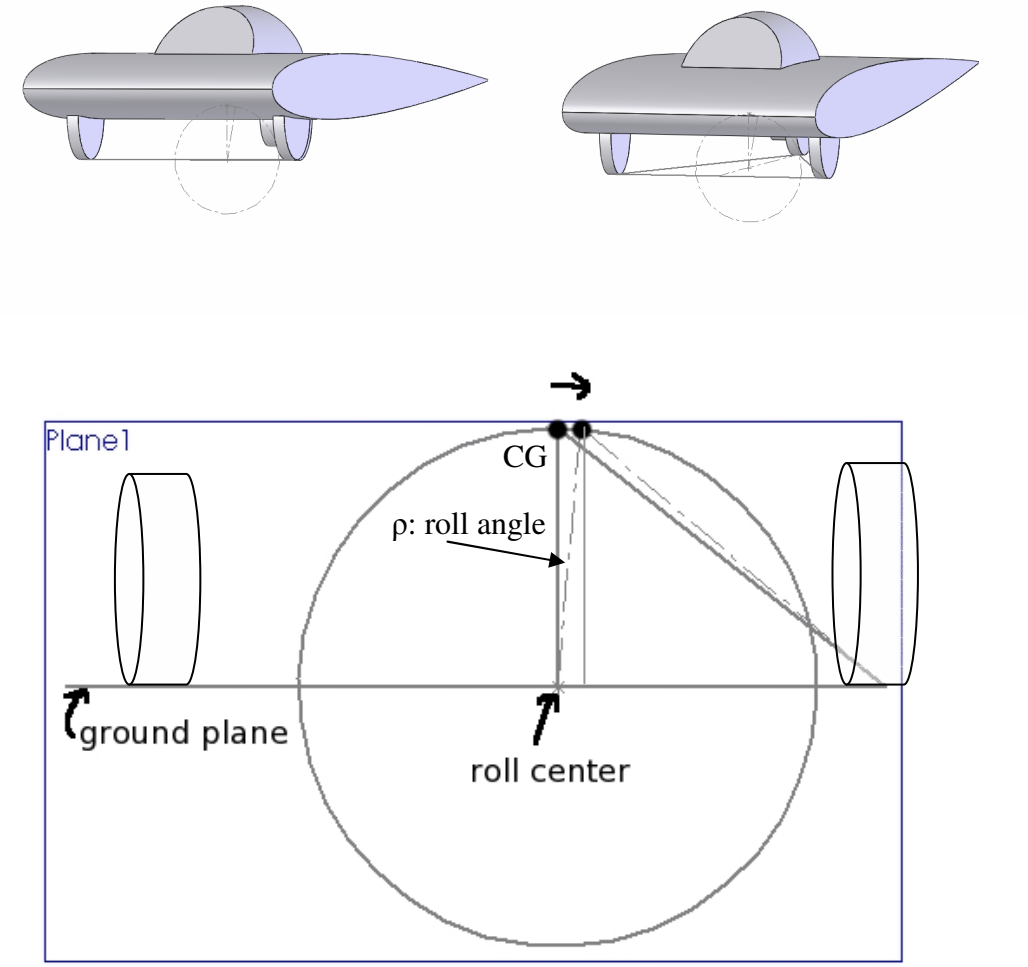

Figure 3.4 Relocation of CG due to roll (view normal to plane 1 of Fig. 3.2)

There is one point to note here, that is the coefficient of friction in the case of starting motion on a gradient must be chosen as low as possible to increase the climbing ability. For example, if the coefficient of friction is selected as 0.4 (μ_{min}) then the car can start moving up the gradient even when the coefficient of friction is as low as 0.4.

Conversely, the coefficient of friction in the case of taking curves must be chosen

as high as possible to decrease the risk of tipping over. Similarly, if the coefficient of friction is selected as 0.95 (μ_{max}) then the car can take the curves up to a corresponding lateral acceleration calculated by the `rollmodel.m` program.

Since these abilities are fixed with the production of the car unless there is a longitudinal weight transferring system, it is better to keep this range as wide as possible. This allows the car to operate on a wide range of road conditions.

3.4 Geometric Verification of `rollmodel.m`

To verify the results of `rollmodel.m`, a sample solution is done by a 3D geometric solver. The input of the program is given in Table 3.7. The results are given in Table 3.8 and Fig. 3.5.

In Fig. 3.5 the 3D configuration is constructed such that the height of CG is equal to length of f. Therefore the `rollmodel.m` file is expected to output a lateral acceleration value of 1g in the stiff suspension case.

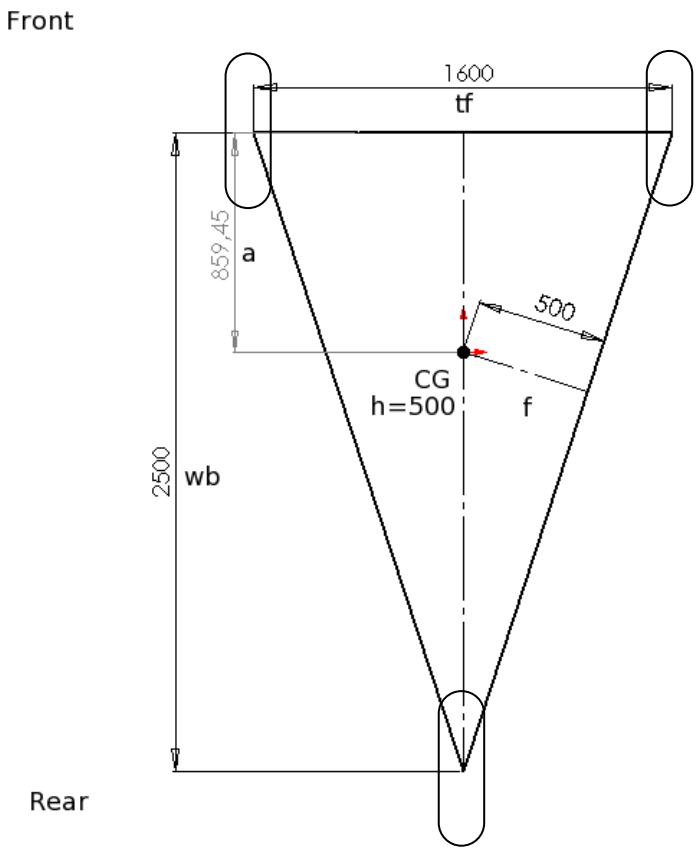

Figure 3.5 Verification setup for `rollmodel.m` (dimensions in mm)
height of CG is 500 mm

Table 3.7 `Rollmodel.m` verification run input	
input:	
wb= 2.5	wheelbase [m]
a= 0.859	a [m]
b= 1.641	b [m]
h= 0.5	height of center of gravity [m]
tf= 1.6	front track [m]
tr= 0	rear track [m]
r= 5	torsional suspension compliance [deg/g]

Table 3.8 `Rollmodel.m` verification run output	
output:	
acc =1.0000	lateral acceleration for tr<tf and stiff suspension
acceleration= 0.916	acceleration corrected taking the roll stiffness into account

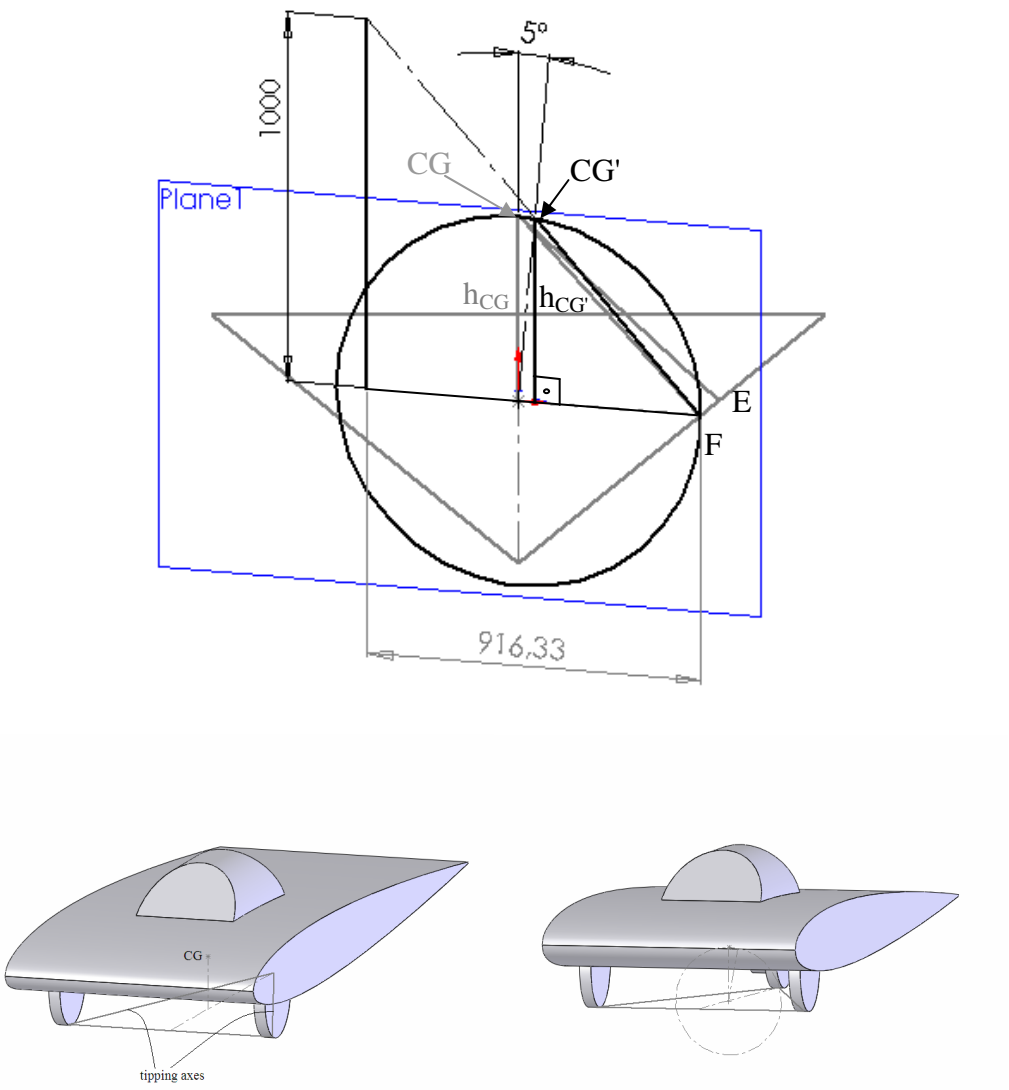

Figure 3.6 Verification setup with 5º roll angle

Table 3.9 `Rollmodel.m` worst case

input:	
a= 1.05	distance of CG from the front axle along the longitudinal axis [m]
b= 1.45	distance of CG from the rear axle along the longitudinal axis [m]
h= 0.65	height of center of gravity [m]
tf= 1.6	front track [m]
tr= 0	rear track [m]
r= 0.05	torsional suspension compliance [rad/g]
output:	
rr= 2.86	suspension compliance [deg/g]
acc= 0.755	limiting lateral acceleration for tr<tf and stiff suspension [g]
acceleration= 0.680	acceleration corrected, taking the roll stiffness into account [g]

The values given above are the safe values for design but the undesired case for a race car. Since these parameters limit the car to worse than its best possible performance. After the design of the car, with realistic values the same programs are run once more.

Table 3.10 `Gradeability.m` with final parameters

Input:	
wb= 2.5	Wheelbase [m]
h= 0.45	height of center of gravity [m]
gr= 0.18	gradient to climb [ ]
mu= 0.5	static coefficient of friction [ ]
power= 3000	motor power [W]
Output:	
max a and min b for front axle driven case	
a= 1.493	upper limit for a [m]
b= 1.006	lower limit for b [m]
max a and min b for rear axle driven case	
a= 0.993	lower limit for a [m]
b= 1.506	upper limit for b [m]
F= 529.7	required force [N]
T= 211.8	required motor torque [Nm]
v1= 5.66	limit speed [m/s]

Table 3.11 `Rollmodel.m` with final parameters

input:	
wb= 2.5;	wheelbase [m]
a= 0.9;	[m]
b= 1.6;	[m]
h= 0.45;	height of center of gravity [m]
tf= 1.6;	front track [m]
tr= 0;	rear track [m]
r= 5;	torsional stiffness of suspension [deg/g]
Output:	
acc= 0.975	lateral acceleration for tr<tf and stiff suspension [g]
acceleration= 0.895	limiting acceleration corrected taking the roll stiffness into account [g]

3.5 Suspension System Selection

For a solar car, expected to cruise at low speeds such as 70 kph maximum and 30 kph on the average, the suspension system is still needed to absorb the shocks when the borders of the curves are used. Additionally, the electronic hardware in the car may be damaged because of the excitations originated by the road surface. Since the excitations caused by the road surface can be assumed to be white noise, there will be excitations at every frequency. Moreover, the tires will be very hard to reduce rolling resistance and therefore will neither act as a spring nor a damper. Therefore in the first design experience, it is too risky to design a car without a suspension system, but with some further investigations it may be beneficial to simplify the design in this direction.

The double wishbone suspension system is chosen for the front wheels and trailing arm for the rear wheel. The double wishbone configuration is the most suitable configuration for the intended purpose of occupying the least space and allowing height adjustment without introducing camber change. Among the few suitable products in the market, the spring damper combination with a spring constant around 100 N/mm is chosen and knowing its stiffness, the geometry is decided on.

Generally the effort goes to having the stiffest configuration possible and the suspension system comes out to be really stiff with 1cm initial and 5cm maximum deflection. Therefore in every other calculation the suspension travel or roll can be neglected safely.

3.6 Results and Discussion

In Table 3.12 using the height of center of gravity *h* and the lowest expected coefficient of friction μ_{min} the minimum value for *a* is read.

In Table 3.13 with the same height of center of gravity *h* and the *a* value taken from Table 3.12 are used together, to get the maximum lateral acceleration μ_{max}.

Table 3.12 "a [m]" the output of `gradeability.m`
Input parameters: h_{CG} (height of center of gravity), μ (coefficient of friction)

μ / h_{CG} [m]	0.4	0.5	0.6	0.7	0.8	0.9	1.0
0.40	1.0705	0.8417	0.6893	0.5803	0.4986	0.4351	0.3843
0.45	1.0613	0.8326	0.6801	0.5712	0.4895	0.4260	0.3751
0.50	1.0522	0.8234	0.6710	0.5620	0.4803	0.4168	0.3660
0.55	1.0430	0.8143	0.6618	0.5529	0.4712	0.4077	0.3568
0.60	1.0339	0.8052	0.6527	0.5437	0.4620	0.3985	0.3477

Table 3.13 "lateral acceleration [g]" the output of `rollmodel.m` with stiff suspension
Input parameters: a (distance of CG from the front axle along the longitudinal axis), h_{CG} (height of center of gravity)

a [m] / h_{CG} [m]	0.35	0.45	0.55	0.65	0.75	0.85	0.95	1.05
0.40	1.4193	1.3624	1.3046	1.2460	1.1866	1.1263	1.0652	1.0031
0.45	1.2819	1.2296	1.1766	1.1229	1.0686	1.0135	0.9578	0.9013
0.50	1.1686	1.1202	1.0713	1.0218	0.9718	0.9211	0.8699	0.8182
0.55	1.0735	1.0286	0.9832	0.9373	0.8910	0.8441	0.7968	0.7490
0.60	0.9927	0.9507	0.9084	0.8657	0.8225	0.7790	0.7350	0.6907

The concern in this chapter is whether the chassis design with 3 wheels will perform safely based on the decision of the location of the center of gravity, single wheel and the motor. In the selected configuration, there are two wheels in front, one at rear. The single wheel hub motor is situated at the rear wheel. This configuration, with height of center of gravity of 0.45 m, has the ability to climb the gradient and take the curves under specified conditions.

On the other hand the same analyses need to be carried out in the case of a chassis with 4 wheels. In that case the minimal track values depending on the height of center of gravity and suspension stiffness can be determined. The position of center of gravity along the longitudinal axis can be decided using the same approach.

CHAPTER 4

DETERMINATION OF THE BODY SHAPE

The body of a car is the covering part on which the air flows. It provides sheltering for the passengers and the other functional parts, against rain, dust and other external factors. In addition to all these, the body of a solar car has to provide an area for the solar panels.

The properties of a desired cover are:

streamlined shape along the direction of flow

light weight

strength to carry the panels and the air load

horizontal panel area, not shadowed by any parts of the car itself

low production cost

The solar panels may have three different bending properties. This leads to different shapes of panel area.

- Type 1 panels: Flat solar panel area, if the panels are brittle and flat.
- Type 2 panels: Cylindrically curved panel area, if the panels can be bent in one direction
- Type 3 panels: Spherically curved panel area, imposes no constraints so that the panels can be freely shaped, i. e. bent in two directions.

Type 3 panels bend in two directions but they have low efficiency (around 8%). In the FIA rules handbook [4] the energy intensity is given as 1000 W/m^2 for the calculations. The allowed maximum power output of the panels is 800W while the incident solar radiation is 1000 W/m^2. This leads to 800 W / 1000 W/m^2 x 8% = 10 m^2 panel area requirement. Since the car dimensions are limited to 5 m of maximum length and 1.8 m of maximum width, even when this area is fully covered with this type of panels, the power output would not suffice. Therefore if the panels of type 2 can be found with sufficient efficiency then it is possible to bend the panel area in the flow direction.

To be prepared for the worst case, the first design was, as shown in Fig. 4.1, with a flat solar panel area.

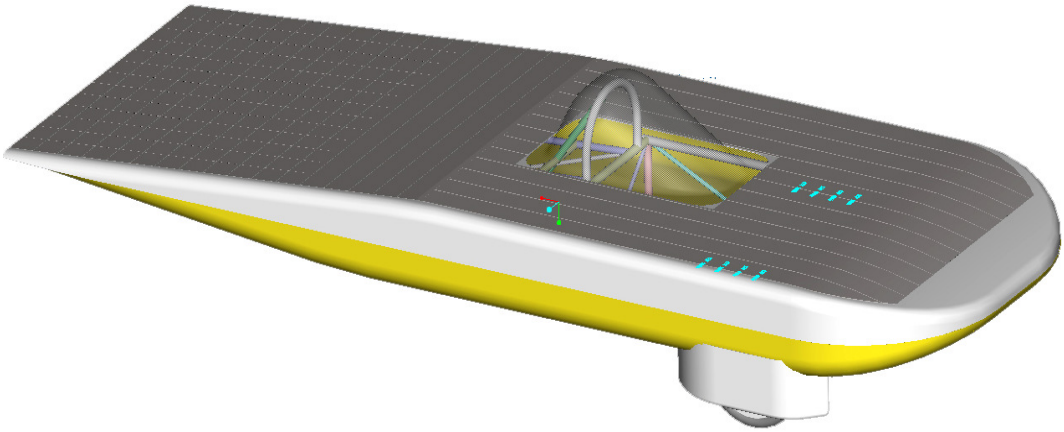

Fig 4.1 One of the previous designs with flat panels (length: 5 m, width: 1.8 m)

In the end of a market search, carried out by other team members, it was seen that panels of type 2 with 13% efficiency could be acquired before the race. Due to 13% efficiency, it is required to have 6.2 m^2 of panel area which is possible within the race rules.

The resistant forces against motion are:

a. dry friction in the joints independent of the speed
b. rolling resistance linearly dependent on the speed
c. aerodynamic resistance dependent on square of the speed

(a.) can be reduced by reducing friction in mechanical design of the joints and improving the quality of materials and manufacturing. This part of the design is carried out by an experienced design engineer and it was very efficient considering the limited budget and time. (b.) can be reduced by using special tires produced for solar vehicles. These tires cause less resistance because there are no tire patterns on them and they can be pressurized to 110 psi. This is a very high pressure level when compared to motorcycle tires with 42 psi of maximum allowable pressure.

4.1 Some Basic Aerodynamics Concerns

The easiest performance gain can be obtained by decreasing the aerodynamic resistance because especially at high speeds, it is the dominating resistance. In Fig. 4.2 the weights are calculated for typical resistance coefficients for solar cars. The lines in the middle represent the result for the original air resistance value. The lower air resistance plot is determined by multiplying the C_d value by 0.8. The higher air resistance plot is determined by multiplying the C_d value by 1.25. The exact values for coefficients used here are not important quantitatively. The important part is to understand the effect. After the design of the car, some values can be expected for the resistance coefficient. The exact values, which are strongly affected by the quality of material and the precision of manufacturing, can be determined by testing.

The performance of the first car can naturally be different from the initial guesses. Therefore, the purpose of the initial product can only be to supply data for improvement of itself or to provide data for the design of the second car. Since the car was produced just before the race and the electronic equipment was not ready by the time, the first year gave little experience and data in this respect.

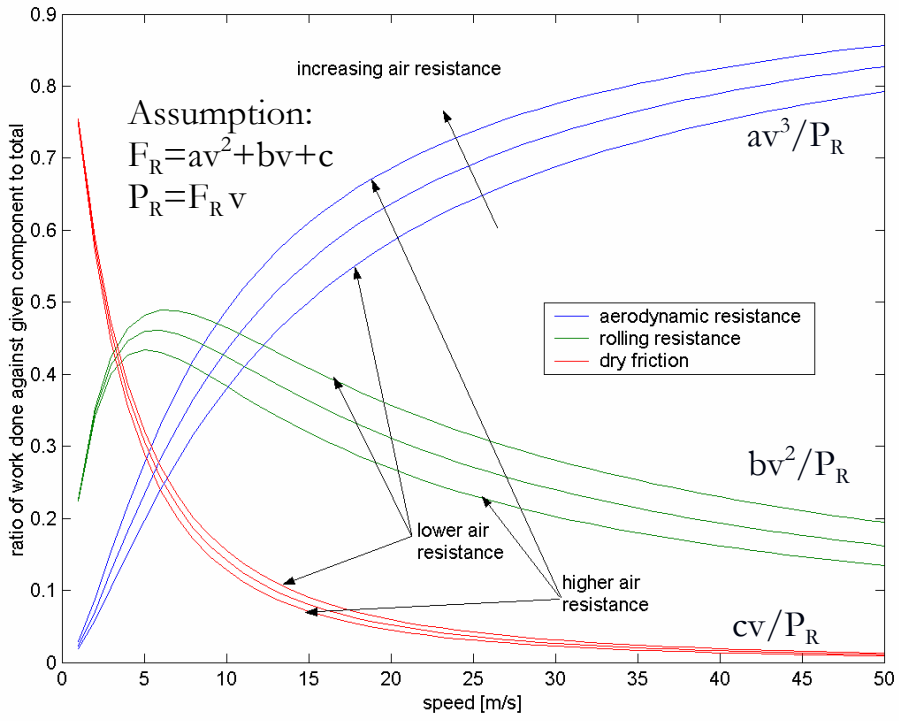

Figure 4.2 Weight of resistances vs. speed

Since the external shape has multiple alternatives within the limits of the regulations, this part of the work allows the team to make difference in designing an efficient race car. In Fig. 4.2 the ratios of work done against each resistance term divided by total resistance is plotted versus speed. Using this plot knowing the speed distribution along the race, the effect of decreasing air resistance can be calculated. For example, in a trip with 15 m/s constant speed, slightly more than 50% of the energy is spent against air resistance. Decreasing this resistance by 20%

will decrease the total resistance by 10%.

Initially it is clear that the body must have smooth contours. Only the functional parts must be allowed to alter the shape. The disturbances created by the parts, such as the canopy and the wheels on this smooth body must be as small as possible. The others must be embedded in the body. The decision that is left to the end is the general shape of the body. The airplane industry has the standardized designs for the wings that are called NACA profiles. For low drag the symmetric NACA profiles are a good starting point. Since they are based on tremendous experience, it is a common practice to adopt one of these profiles whenever they might be useful. [16]

4.2 Effects of Production Capabilities and Limited Budget on Body Shape

Since the design will be realized with a limited budget and production capabilities, the limitations were investigated beforehand and it was seen that the body, which consists of upper and lower shells, must be symmetric about the horizontal plane. This would decrease the production cost by requiring a single mold. The upper half could be weaker than the lower half because the loads on it are weight of the solar panels and the air pressure forces. The lower half was attached to the chassis and the loads on it were the upper shell with panels on it and the air forces. Therefore first half shell would be tested in strength and the second would be built lighter if the first one is strong enough. In case the first half shell is found to be weaker than expected, then it would be used as the upper half shell. Therefore there is no waste of material, time or money.

One last constraint coming from the production capabilities was to build the shape over 2D slices, using wooden sheets that bend in one direction. That was because of high cost of a 3D mold machined by a CNC. The 2D slices would be cut by

laser using cheaper material and less time in a simpler machine. Then several identical profiles are placed with equal distance to form the base of the mold. A wooden sheet is laid on the surface created by the ends of the profiles.

Considering these production ability constraints together with aerodynamics concerns, the shape was already clear. There were not many options left but extruding a symmetric NACA profile along the width of the car and placing the wheels and the driver into smallest and the smoothest possible disturbances from the shape.

4.3 Safety Measures

Safety of the driver had a high priority in both the design and the construction of the car. The rules already imposed active safety measures, such as dual-circuit braking system requirement, and passive safety measures, such as roll bar requirement [4].

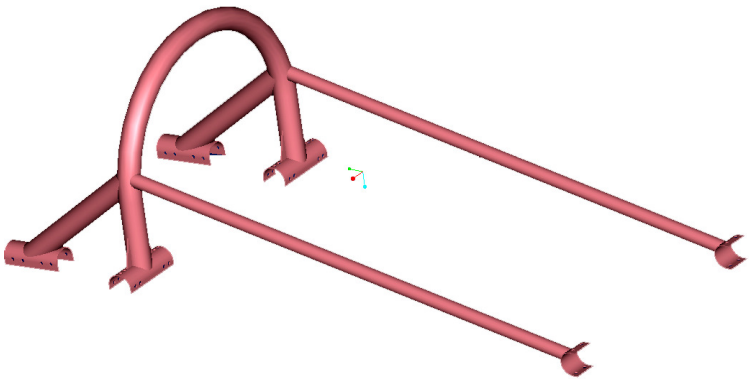

Figure 4.3 Roll bar

Besides conforming to the rules, the car has additional safety measures. There is a zone in front of the car where the carbon fiber body can easily deform or brake.

The chassis is 40 cm behind this outer structure. Additionally the body is attached to the chassis with deformable aluminum plates and this allows the body to move a few centimeters without taking damage in case of a slow contact. Although the motion of the body is limited with 40 cm on the chassis, for increased safety the roll bar has frontal extensions to direct the body upward, over the helmet of the driver to decrease the risk of injury by the sharp broken parts of the brittle layer. Longer bars to the right of the figure in Fig. 4.3. Considering the high brittleness of the carbon fiber layer, the region surrounding the driver is coated with an additional less brittle Kevlar layer.

4.4 Computational Fluid Dynamics (CFD) Analyses

After deciding on the shape, the next step is to analyze the aerodynamic behavior of this shape and to obtain the aerodynamic drag coefficient which is used in the dynamics chapter (Chapter 5).

In the aerodynamics analyses commercial softwares Gambit and Fluent were utilized. Gambit was used to create the mesh in the domain. Fluent is the finite volume Navier-Stokes solver.

The computational domain (Fig. 4.4) has a length of 50 m (10 x length), width of 9 m (5 x width), height of 5 m (8 x height). The vehicle is situated after 5 m (1 x length) from the beginning therefore the downstream has a length of 40 m (8 x length).

The mesh type is selected as tetrahedral because of the surfaces in hand. Most of the surfaces have triangles with small angles; especially, the profile becomes very thin in the rear end of the body. A structured mesh would produce cells with high skewness in locations close to these sharp ends.

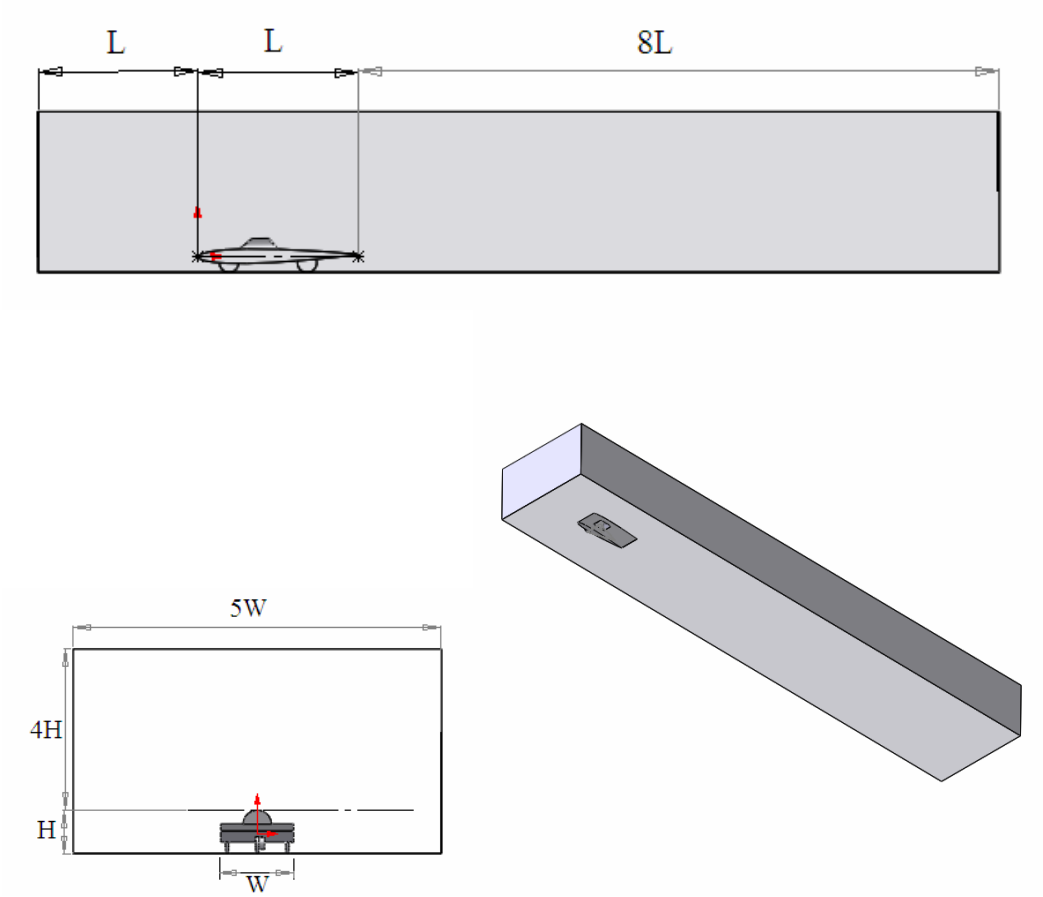

Figure 4.4 The vehicle location in the wind tunnel
Top, side view (not to scale)
Bottom left, rear view (not to scale)
Bottom right, scaled isometric view

To control the size of the cells, a size function is created in Gambit such that the start size on the vehicle surface is 4mm. Consecutive cells grow with a factor of 1.2 and growth continues up to 3 m where the cell size reaches to 1.5 m.

The reason for such a small (4 mm) cell size in the beginning is excessive skewness of cells on the surfaces with sharp ends. The constraint of having no cell skewness worse than 80% requires this small size.

The growth factor of 1.2 is the practical upper limit. Higher growth factor leads to

skewness of cells because the consecutive cells change rapidly in dimensions. The largest practical value for the growth factor is selected because the initial size is already small compared to any details on the car. Smaller growth factor leads to large number of cells exceeding the limitations in memory size. These parameters gave the smoothest solution with manageable number of cells. More cells or finer mesh led to swapping which adds very long hard disk access time when compared with the processing and RAM access time. Less cells or coarser mesh gave less accurate result in nearly the same time. The finer and coarser mesh parameters are given in Table 4.1 for comparison.

Table 4.1 Size function parameters

	Coarser Mesh	Preferred Mesh	Finer Mesh
Start Size [mm]	4	4	4
Growth Rate	1.20	1.20	1.18
Distance [mm]	2 000	3 000	3 000
Max Size [mm]	2 000	1 500	1 400
#cells	1 381 900	1 416 495	1 814 871

4.5 Solution and Results

The CFD analyses were carried out in this chapter to get the C_d value of the body. It would be used in the dynamics chapter and would constitute one of the three loss coefficients. In fact these analyses could be used to optimize the shape of the car, but the shape is already fixed by the previously imposed non-technical constraints. The only variable is the height of the profile and it is chosen as the slimmest possible value, which makes the body cover the driver and the chassis around. It came out to be 45 cm in the highest point with 5 m of length which is denoted as NACA0009, Fig 3.1. The first zero “0” stands for no camber (symmetric profile), the second zero denotes the position of camber and the “09” stands for the aspect ratio 0.45 m / 5 m = 9%.

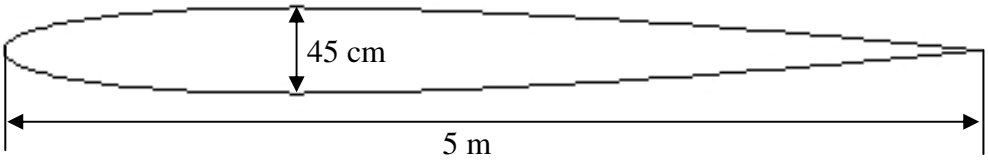

Figure 4.5 NACA 0009 profile

The Boundary Conditions are:

- uniform prescribed velocity profile at the inlet
- stationary vehicle
- tunnel walls and the road (bottom wall) moving with the speed of the flow
- atmospheric pressure at the outlet

Turbulence model is selected as RKE (Realizable k-ε) as suggested in the study "Computation of Drag Force on Single and Close-Following Vehicles" [17]. Similarly Non-equilibrium Wall Function is preferred instead of Standard Wall Function as pointed out in the same study.

By giving these constraints and selecting the solution methods as the second order upwind for all properties except for the pressure-velocity coupling where the SIMPLE method is used. The solution is repeated for 3 different speed values of 10, 15 and 20 m/s.

Windy conditions can also be simulated if needed. Then the moving wall velocity will be different from the inlet velocity. This would also yield the solution for a car moving in a tunnel. If the tunnel effect needs to be eliminated, then the

computational domain needs to be larger and the bottom wall (the road) must be separated from the side walls. The side walls move with the flow, and the bottom wall moves with the speed of the car, whereas the car is fixed in the tunnel.

The results of the runs to check for grid independence are given in Table 4.2. The test speed is selected as 15 m/s which corresponds to 54 km/h.

Table 4.2 Comparison of the results to check for grid independence comparison case: Hasat 1A 15 m/s

	C_d	C_d x A_{cs}
Coarser mesh	0.339	0.382
Preferred mesh	0.344	0.389
Finer mesh	0.320	0.362

One other helpful use of the program may be on investigation of drift effect [17]. For this, two cars following each other with a certain distance and maybe with some offset can be modeled. Then the decrease in drag force, the amount of power saving due to drift can be estimated. It is obvious that for successfully designed solar cars, traveling at low speeds this effect will not be significant. Furthermore there are some limitations on following the other cars closely. Its effect may not be beneficial in the end, because the car followed may not travel at the optimal speed for the following car. The optimal speed will be discussed in the following chapter.

The analyses for preferred mesh are repeated 3 times for 10, 15 and 20 m/s cases for 3 different geometries. The differences in the geometries are due to the changes in canopy.

The version of Fluent™ software output the total forces on selected surfaces. C_d values are calculated using these outputs from

$$F = \frac{1}{2}\rho A C_d v^2 \tag{4.1}$$

Therefore,

$$C_d = \frac{2F}{\rho A v^2} \tag{4.2}$$

The resulting drag coefficients are tabulated in Table 4.3.

Table 4.3 Drag coefficients with respect to speed

C_d	10 m/s	15 m/s	20 m/s
hasat1a	0.366	0.344	0.334
hasat1b	0.270	0.321	0.240
hasat w/o canopy	0.253	0.269	0.296

And the real target value to minimize, which is the drag coefficient times the cross sectional area, is given in Table 4.4. This is the value to minimize because these are the values related with the geometry of the car. If minimizing only the air drag coefficient requires some increase in the cross sectional area, then this may not really lead to minimization of the drag force.

Table 4.4 Drag coefficients multiplied by the cross sectional area with respect to speed

C_d x A_{cs}	10 m/s	15 m/s	20 m/s
hasat1a	0.414	0.389	0.377
hasat1b	0.294	0.350	0.262
hasat w/o canopy	0.233	0.248	0.272

The total pressure is selected as the first figure because it is the quantity demonstrating where the fluid is energized. The aim of the low drag design can be stated as creating as small difference as possible in the total pressure figures,

behind the car. There is one point to note in the figures. The total pressure (contours shown in Fig 4.6) decreases in the flow where it is disturbed and takes energy from the car, whereas it must be increasing behind a moving car. Remembering the fact that, this is a tunnel model, the car is stationary and it can only stop or slow down the flow.

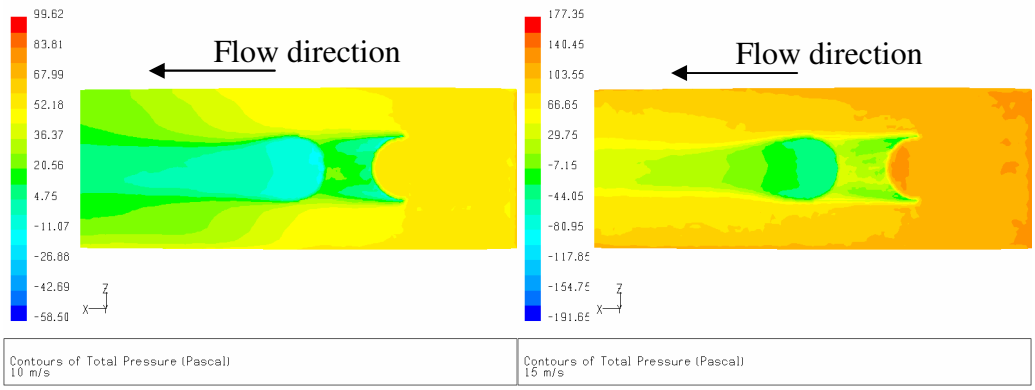

Figure 4.6 contours of total pressure, car is viewed from top
left: flow speed is 10 m/s
right: flow speed is 15 m/s

As can be seen in Fig. 4.7, the velocity change due to the car diminishes and the flow reaches its original velocity in the virtual tunnel, in less than 5 m (the length of the vehicle) downstream. This means after less than a car length there is no energized flow by the car. Since energizing the fluid means losing energy for the car, this is an indication of good design. This also shows that the drift effect is negligible. In other words, following the car in front closely, to increase the speed, by decreasing the air drag will not be effective. In most cases, this is risky and in such a race with frequent accelerations and decelerations it must not be considered as an energy saving method. In Fig 4.7 left, it seems that the flow is energized more, but it is due to the high sensitivity of the contours because the pressure range is very narrow on this figure.

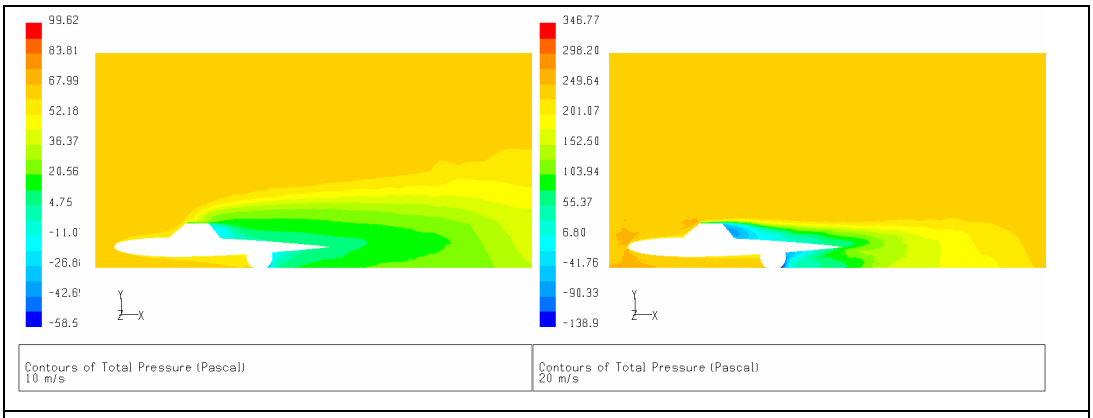

Figure 4.7 Contours of total pressure on the symmetry plane

In Fig. 4.8, the static pressure distribution on the car is shown with the old and the new canopies. Such an illustration is useful while determining the air inlet and outlet locations. The inlets must be located at the regions with higher pressure and the outlets must be at the regions with low pressure. Locating the air inlets and outlets correctly provides more effective cooling or air circulation while causing less additional drag. However, cooling is not generally required and better aerodynamic performance is preferred.

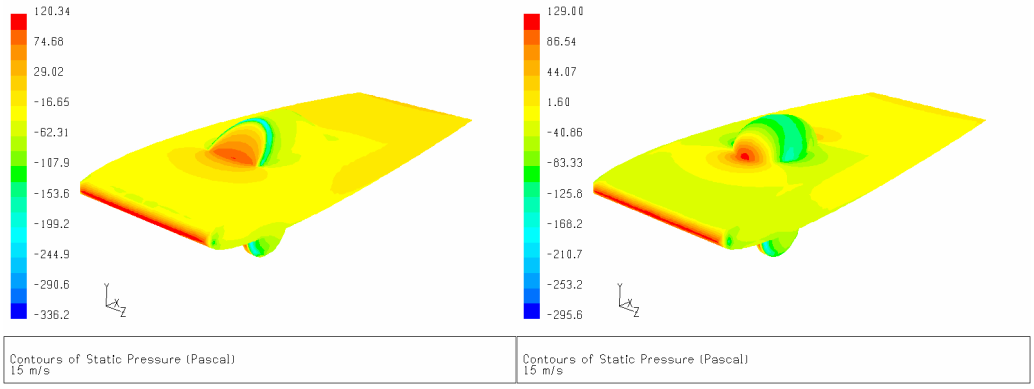

Figure 4.8 Static pressure (gage) contours on the car
Left: Hasat 1A with the old canopy
Right: Hasat 1B with the new canopy

In the end of these CFD runs and considering the results obtained in [17], it is seen that the results of wind tunnel experiments are still vital to check the accuracy of

C_d values obtained from CFD analyses for flows with separation. As stated in [17], the flow models may still give inaccurate results especially when separation occurs. Therefore CFD runs can only be used with the help of some reference values measured in the wind tunnel tests for the same geometry. The realizable k-ε turbulence modeling is used as advised [17]. Especially when separation bubble is formed on the body, the realizable k-ε method gives more accurate results when compared to standard k-ε and k-ω which predict higher drag coefficients [17].

CHAPTER 5

RACING STRATEGY

5.1 Determining the Strategy to Drive the Car through the Course

The driving strategy during the race is a multiplier of the final result; i. e. the car may be designed and constructed perfectly, maybe with unlimited resources, but it must also be driven carefully to achieve the desired results. This needs thorough understanding of sources of energy losses during the race. The car is designed to minimize these losses within the production capabilities but in the beginning of the race, it is a car with fixed loss coefficients of resistant forces.

5.1.1 Longitudinal Performance

During traveling, the energy stored in battery is used to do work against the gravitational force and the frictional forces. Since the work done on gravitational force is zero on a closed circuit the only concern in this race is the frictional forces. For simplicity these forces can be labeled for easier reference as:

$$F_R = F_a + F_b + F_c \tag{5.1}$$
$$F_a = a_0 v^2$$
$$F_b = b_0 v$$
$$F_c = c_0$$

$$\sum x = v_1 \Delta t + v_2 \Delta t + v_3 \Delta t + ... + v_n \Delta t \tag{5.2}$$

Having constant total distance to travel $\sum x$ with constant Δt intervals

$$\sum x = \Delta t \sum v \tag{5.3}$$

So that, the term $\sum v$ is constant

$$\sum v = v_1 + v_2 + v_3 + ... + v_n \tag{5.4}$$

in the case of cruising with constant speed

$$v_1 = v_2 = v_3 = ... = v_n = v_0 \tag{5.5}$$

$$\sum v = nv_0 \tag{5.6}$$

- F_c independent of speed
- F_b linearly dependent on the speed
- F_a dependent on square of the speed

Work done against F_c is

$$W_c = F_c \sum x \tag{5.7}$$

the remaining terms depending on speed can be given as

$$W_a = \sum F_a v \Delta t = \sum a_0 v^3 \Delta t \tag{5.8}$$

$$W_b = \sum F_b v \Delta t = \sum b_0 v^2 \Delta t \tag{5.9}$$

$$W_a \propto \sum v^3 \tag{5.10}$$

$$W_b \propto \sum v^2 \tag{5.11}$$

Suppose that in a time interval of Δt the speed v_1 is kept constant at $v_0 - \delta$ and to make up for that lag v_2 is kept constant at $v_0 + \delta$ and the remaining distance is traveled with v_0.

$$\sum v^2 = (v_0 - \delta)^2 + (v_0 + \delta)^2 + (n-2){v_0}^2 \tag{5.12}$$

Rearranging,

$$\sum v^2 = {v_0}^2 - 2\delta + \delta^2 + {v_0}^2 + 2\delta + \delta^2 + (n-2){v_0}^2 \tag{5.13}$$

$$\sum v^2 = n{v_0}^2 + 2\delta^2 \tag{5.14}$$

Similarly for the third order dependence on speed

$$\sum v^3 = (v-\delta)^3 + (v+\delta)^3 + (n-2)v^3 \tag{5.15}$$

$$\sum v^3 = v^3 - 3v^2\delta + 3v\delta^2 - \delta^3 + v^3 + 3v^2\delta + 3v\delta^2 + \delta^3 + (n-2)v^3 \tag{5.16}$$

$$\sum v^3 = nv^3 + 6v\delta^2 \tag{5.17}$$

The additional term $2\delta^2$ is for the second order dependence on speed and $6v\delta^2$ is for the third order dependence on speed. These terms are always positive and the magnitudes increase with increasing diversion from the average speed. Similarly each fluctuation in speed produces more from the same terms.

If the compensation is done in more than 1 time interval, where "n" is the number of the interval the compensation is realized

$$\sum v = (v_0 - \delta) + (v_0 + \frac{\delta}{n-1})(n-1) \tag{5.18}$$

$$\sum v^2 = (v_0 - \delta)^2 + (v_0 + \frac{\delta}{n-1})^2(n-1) \tag{5.19}$$

Then the additional term becomes $\delta^2(1+\frac{1}{n-1})$ and this tends to δ^2 when n is large. This shows that, when there is an error in following the target speed the correction must be done in as long time as possible.

Therefore the work done against these forces needs to be minimized while maximizing the average speed. The optimal strategy is given in [18-22] as holding the speed constant. The difference between this thesis and the referred ones is that,

they operate on complete models, therefore make more complex analyses but still find out that keeping the speed constant is the best strategy. In that sense, the simple reasoning given above is more comprehensive.

As a result of this approach the optimal strategy comes out to be cruising at a constant speed. Then the following step is to determine that constant speed. With uncertainties in solar energy available during the race, some adjustments may be required.

The ideal battery assumption, meaning that the battery supplies a fixed amount of energy under all power supplying conditions, leads to a conclusion advising that keeping the speed constant throughout the race is the best strategy. From the electrical point of view it can be shown with a similar method as above that the energy output of the battery can be maximized by drawing constant current from the beginning to the end of the race. The ideal solution is somewhere in between these two enveloping solutions. Therefore the strategy is selected as maximum power below some speed (v_{min}), no power above some speed (v_{max}) and linear interpolation in between. This is both close to speed holding strategy and sensitive to battery characteristics.

Using Li-Ion batteries has never been considered due to safety reasons [23] and Lead-Acid batteries can be considered to be very close to the ideal case, C type of driving input in Fig. 5.1 is considered to be good enough. The optimal value for v_{max} - v_{min} can only be found knowing the discharge efficiency of the batteries depending on the power withdrawn.

5.1.2 Handling Performance: Definition of Ideal Race Line

Taking curves has always been a challenge. Nearly on all the races (except for drag races and speed record trials), each driver tries to show that he can act as the best

controller to take the curves. Therefore, the races are conducted on tracks with various curves.

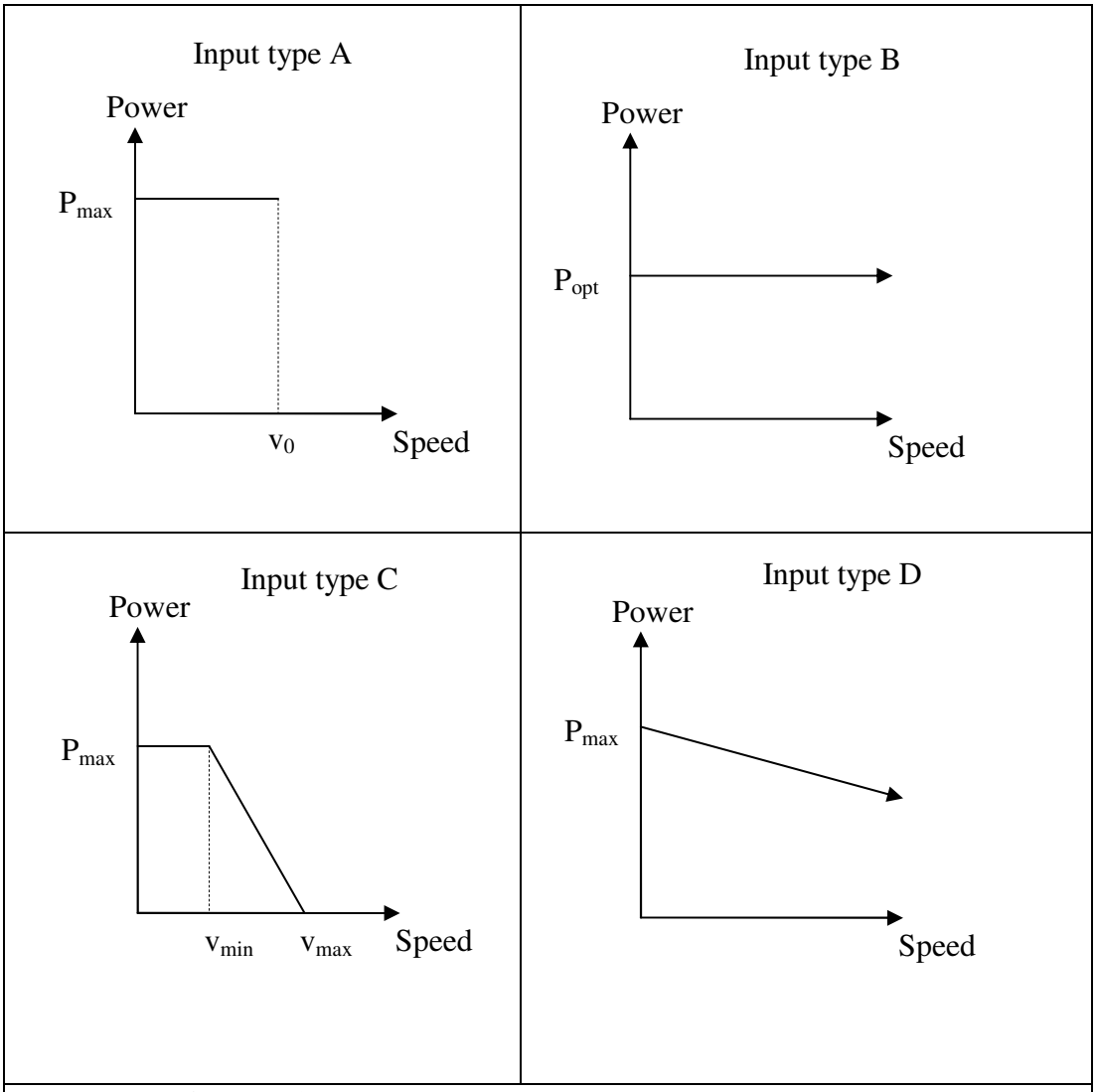

Figure 5.1 Alternatives of power input depending on speed

There must be a unique, optimal route to follow for any given track, to minimize the time to complete the lap. The aim is to keep the high speed gained on the straights as much as possible. The best route is the one that allows the highest speed, but it might be too complicated to determine. Intuitively, a good assumption

is that the route is composed of straight lines on the straights and arcs with constant radius of curvature on the curves. That means the ideal route on the curves will be circular. This simplifies the problem. Because the path is composed of straights and circular curves, but how these fit in the course of the racing circuit is a geometric problem and can be described as follows; draw a circle which is tangent to outer line of the incoming straight, tangent to inner curve and tangent to outer line of the outgoing straight. This is the circle with largest possible radius of curvature as demonstrated in Figure 5.2. But this solution is valid for a point object. Since the car has a finite track width, the borders of the track must be offset towards the inside in order to reflect the real boundaries the center of gravity can follow.

The width of the straights and the curve can vary. Actually the width of the road does not affect the shape of the ideal line as long as the borders in contact with the line remain the same.

One other point is that the shape of the track does not need to contain only basic geometric shapes, such as perfectly linear straights and circular curves. The track in question may have arbitrary shapes, but the ideal line must consist of circles with largest possible radii of curvature and tangent lines between them. Tangency is strictly required since the radius of curvature on a broken line is zero “0”, it is only possible to follow a broken line by stopping the car and that is out of question while looking for the fastest route.

The given explanation is for a curve between two sufficiently long straights. It demonstrates the idea (Fig. 5.2) but if there are two or more consecutive curves with short straights in between, such that the circles created for the curves intersect. Then the aim is the same but the previous approach does not work. Because the ideal line turns out to be broken, as shown in Figure 5.3, whereas it needs to be continuous.

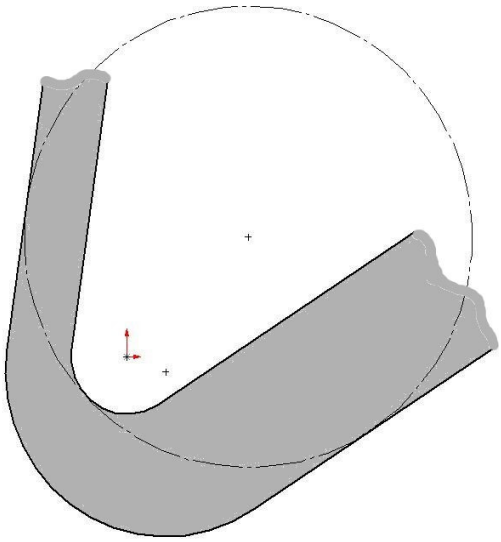

Figure 5.2 Ideal line in an arbitrary curve

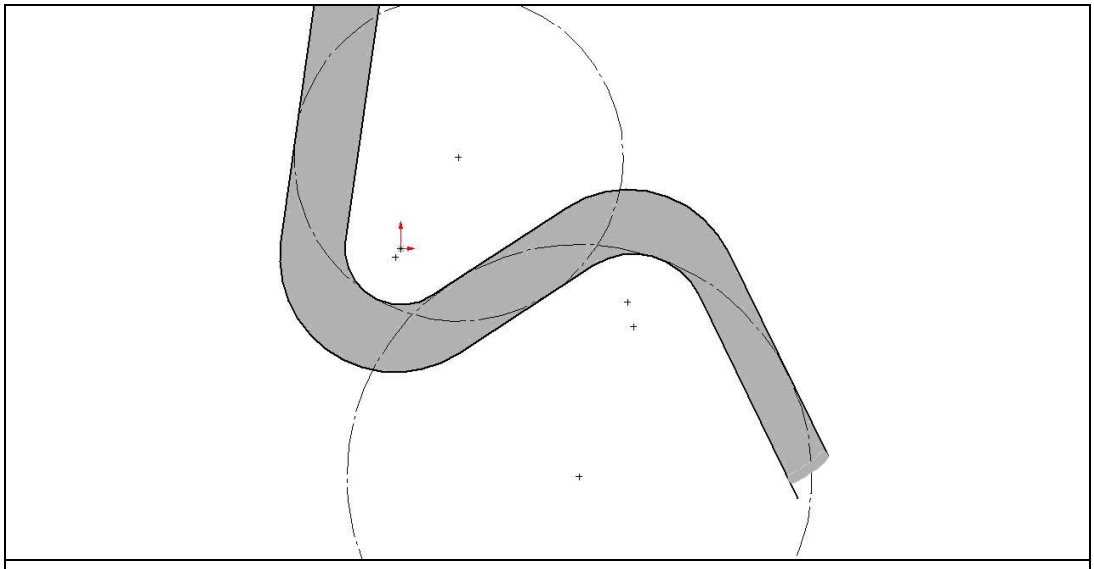

Figure 5.3 Failure of simple definition in compound curves

This time, the constraints imposed to fit the circles become;

- first circle tangent to outer line of the incoming straight
- first circle tangent to inner border of the first curve
- first circle tangent to second circle

- second circle tangent to inner border of the second curve
- second circle tangent to outer line of outgoing straight

With these constraints there is still one more degree of freedom for the circles. To obtain a unique path, there must be one more constraint and that comes from the physics of the problem. Since the car needs to have constant speed during cornering, the allowable speed and therefore the radii of curvature of the circles must be equal. For this solution, a drawing program with dynamic solver is utilized. As a result of this correction Fig. 5.4 is obtained. This race line must always be checked. If the race line goes out of the track in any part of the circuit, then the solution needs to be revised.

As can be seen in the constraints, the problem is symmetric and the ideal line does not have a direction. In both directions the same path is ideal.

The car ideally follows this path. It may take the curve with maximum allowable speed, or with its speed limited by other means if the lateral acceleration to take the curve is below the critical level for the corresponding curve.

The definition of ideal line is given here for convenience; misconceptions about the definition would lead to misunderstanding on many discussions throughout the text. Since the definition of the ideal line is considered as common knowledge, no references are given.

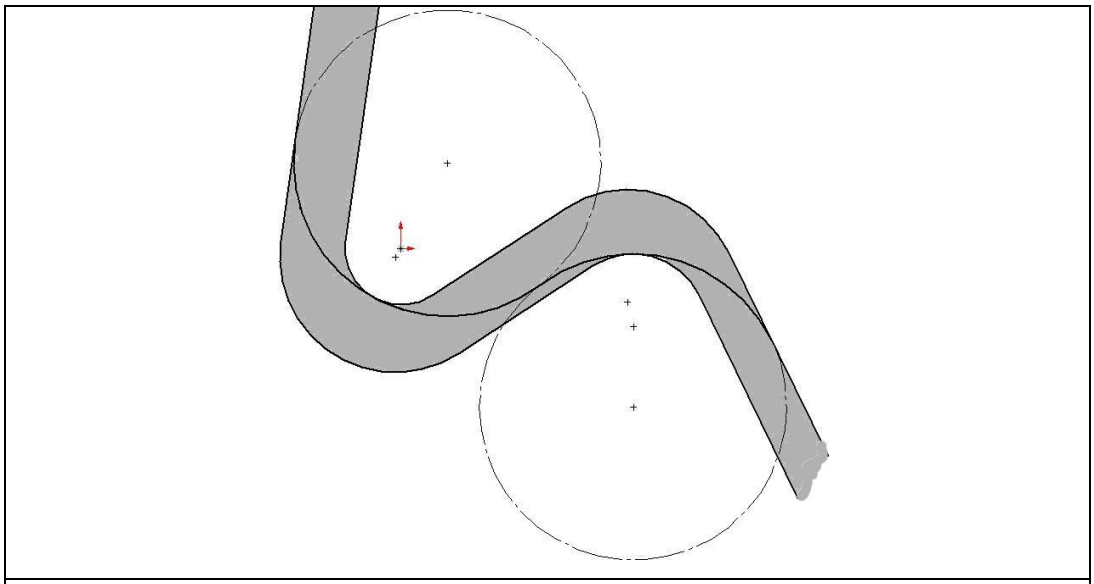

Figure 5.4 Definition of ideal line modified for compound curves

5.1.3 Weighted Average Speeds

To simplify the problem, the straights and simplified curves are added together and the lap time is calculated. Since there are too many interdependent parameters in this problem it is not easy to optimize all the variables.

The properties describing the car in dynamics point of view are as follows:

- dimensions of the car (width, height, length)
- position of CG in 3 dimensions
- number of wheels, number of motors and their placement
- air drag coefficient
- tire rolling resistance and viscous friction coefficient
- dry friction coefficient
- wheelbase
- track

Therefore it is sufficient to create one solution that is good enough, not the ideal one. The ideal solution requires repeated iterations of dynamics and aerodynamics optimizations. Every change in the design leads to another optimal driving strategy. Simulating with the chosen parameters and estimating the result gives data to optimize further. For example the most important speed for the aerodynamics design is obtained.

"The most important speed" can only be obtained having the complete lap data and utilizing the following tools.

Some weighted average speeds need to be defined here.

- Average of w_0 (w0mean): note the speed in constant time intervals, sum them up and divide by the number of samples. This gives the average speed (w0mean). Literally, for how long time the car traveled at that speed. The distribution of data will give at which speed the car travels for most of the time.
- Average of w_1 (w1mean): take the same array w and multiply every element of it by the speed to see the weighted average at which speed the car travels. This is the same with the w0mean when the car travels at constant speed and larger than that if the speed changes in a wide range. Literally for how long distance the car traveled at that speed.
- Average of w_2 (w2mean): repeat the same calculations for w2mean but this time multiply elements of w with v^2. Find literally, how long the car traveled against what force in one complete lap.
- Average of w_3 (w3mean): lastly and the most meaningfully multiply w with v^3 and find the mean power consumption speed, in other words the average speed to make the car consume the same amount of energy during the lap. The distribution gives at which speed the car spends its energy during the lap.

Remembering the fact that for the highest average speed (since the race length is constant, this corresponds to the quickest finish) having a constant speed which is equal to the average speed is the most efficient way of spending the fixed amount of energy. The distribution of these quantities on the speed range is plotted for first two laps in Istanbulpark and given in Fig 5.5.

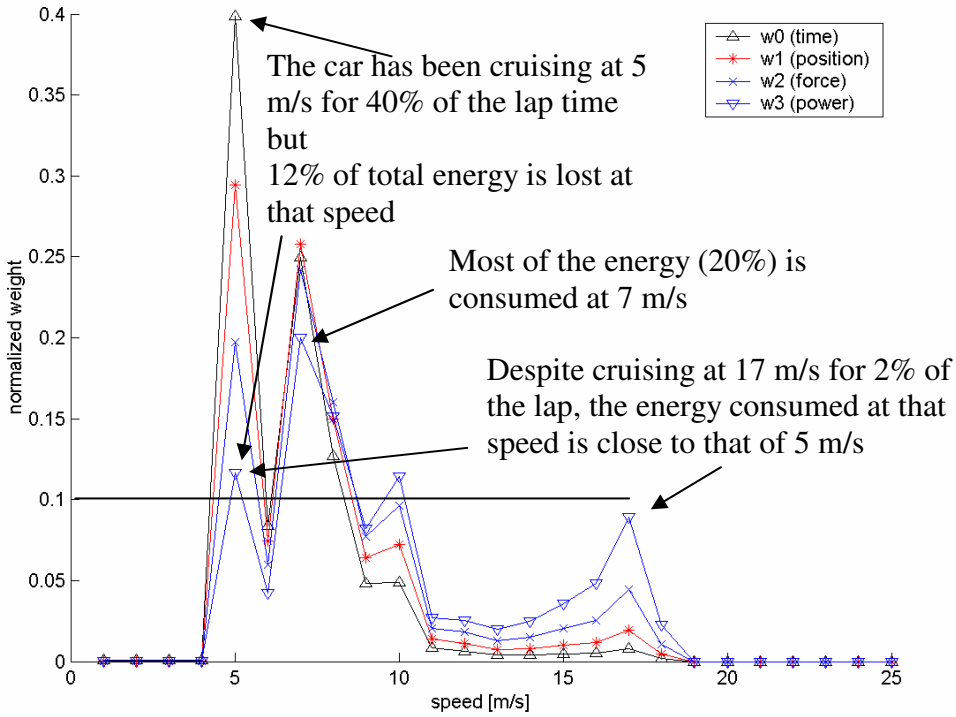

Figure 5.5 Distributions of w_0, w_1, w_2 and w_3 vs. speed in the first two laps

As shown by the equations from 5.1 to 5.17 even gradients, either uphill or downhill, must not affect the speed because total work done against gravity is zero around a closed circuit. But there are two issues to discuss about gradients.

a. Uphill gradients may require very high power to keep the speed at the prescribed value: There is a similar problem for the power output of the batteries. From the electrical point of view, supplying same power throughout the discharging period is the most efficient way of discharging. Therefore it may not be the best strategy to overload the batteries to keep the

speed constant. Taking this into account the power output is limited and controlled depending on the speed.

b. Downhill gradients may cause higher speed than intended: In this case, an option is to use regenerative braking. By the way, the excess energy can be stored to use later, then the efficiency of regenerative braking must be known. To be able to decide, quantitative results are required and they can only be produced after all the parameters are fixed.

5.2 Determining the Telemetry Data and the Limits for the Car

Since there are no slopes steeper than 8% on the circuit, there is no need to exceed the 18% grading ability required by FIA rules and regulations. This ability will allow an acceleration of 1.8 m/s^2 on level road. This is reasonable, keeping in mind that the torque is limited and the power is determined by the speed therefore the acceleration can be kept constant up to the desired speed. Generally the desired speed is fairly lower than the maximum speed limited by power. Limiting the acceleration to 1.8 m/s^2 means, putting the center of gravity as close to the front wheels as possible. This makes the car more stable against tipping while cornering.

The telemetric data calculation is carried out by the `dynamics08.m` Matlab m-file. This file is included in the appendix. Some of the resulting graphs for a sample run are given below. By the help of `dynamics08.m` the position, speed, acceleration, power consumption, torque requirement can all be displayed versus time and this brings the ability to complete virtual laps with the car.

The total energy available for the race is estimated to be 1800 Wh. The energy supplied by the batteries is assumed to be 800 Wh because the 1000 Wh capacity label is valid for a discharge period of 5 hours. In the case of discharging in 2 hours, the available energy is estimated as 800 Wh by the related team member. The energy supplied by the solar panels is estimated as 500 W for 2 hours giving a

result of 1000 Wh, considering the absence of a peak power tracker and several measurements done by the other team members.

5.3 `Dynamics08.m` MATLAB™ Program

Dynamics08.m is a multi purpose program simulating a full lap on the Turkish Formula 1 track, Istanbulpark. The inputs are the weight of the car, the resistance coefficients and the motor characteristics. The outputs are the position, velocity, acceleration, power consumption versus time. Since all these are calculated for any time of the race, other outputs that are functions of the given properties can easily be integrated into the program. This program can also be used to calculate the effects of any change on the car to the lap time. The other very useful outputs of the program are the weighted speeds.

5.4 Results

Calculation of the average speed of the race, knowing the resistant forces and the total energy available is carried out in this chapter. Actually the calculation carried out for this, gives more than that single value. It supplies a complete lap's telemetry data for the first and the following laps. Even various scenarios can be foreseen and can be prepared for any unexpected event during the race. The importance of knowing the average speed or the lap time is the key factor in increasing the overall success in the race. If the driver can be told the new optimal speed because of the changing conditions then the optimal strategy in the rest of the race is cruising at the newly calculated speed considering the remaining battery capacity and the remaining time or laps to go.

The following graphs given in Fig. 5.6 and Fig 5.7 display the selected variables versus time and position respectively. Time axis starts from the lap start where car is at rest and lasts for two laps. Start of the second lap is indicated on the figure.

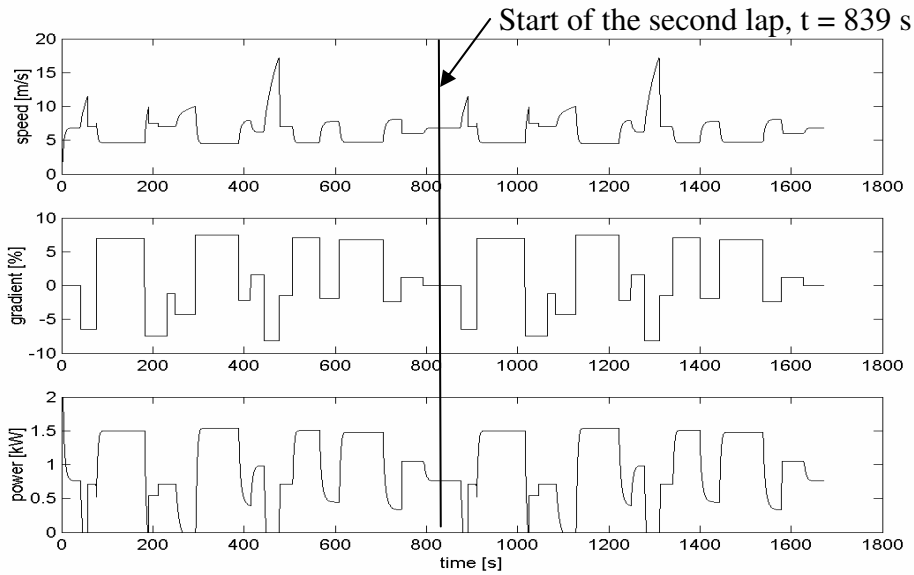

Figure 5.6 Speed, gradient, power vs. time plots during 2 laps

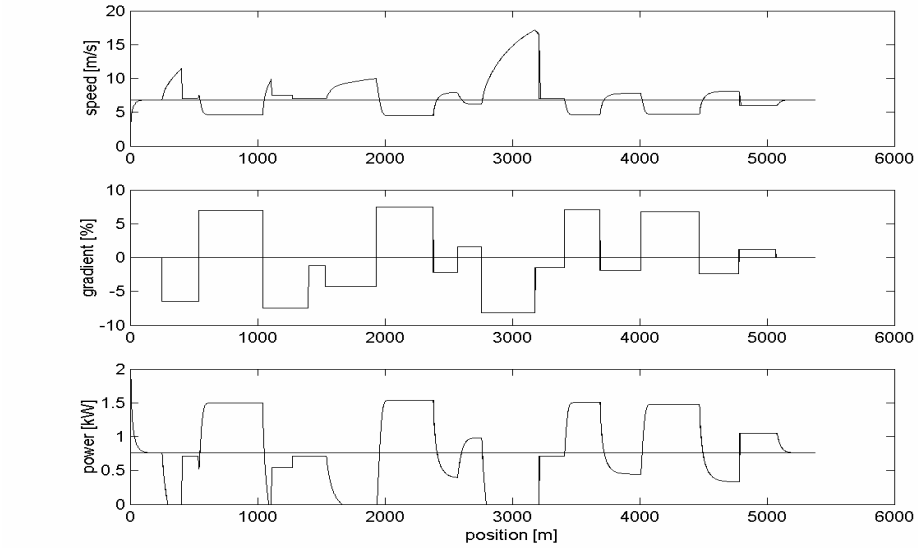

Figure 5.7 Speed, gradient, power vs. position plots

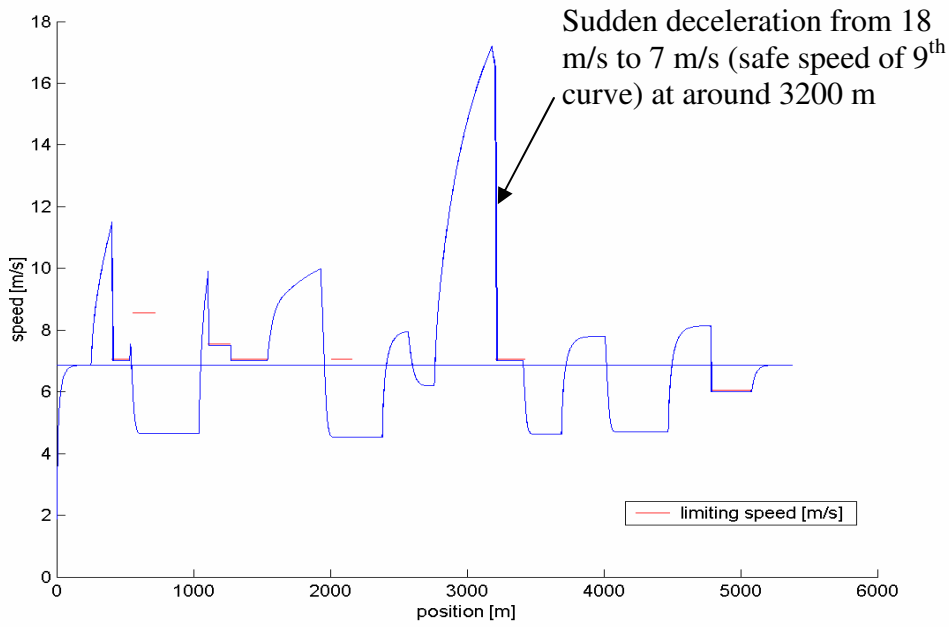

Figure 5.8 Effect of curves on speed vs. position plot
Sudden decelerations to limiting speeds of corners, labeled red, are cause of waste of energy.

Table 5.1 Effects of changes on laptime and energy consumption
(values that belong to standard case are in bold type)

case	input:	output:
standard	M=330; % [kg] dt=0.2; %[s] afr=0.5*1.25*1.13*0.40; % [kg/m] bfr=2.5; % [kg/s] cfr=80; % [kg*m/s/s] fcorsafe=0.5 (factor of cornering safety) power=2000; [W] powcoeff=max(min(3,0.5*(9.14-v(i))),0)/3	vmean =**6.4119 km/h** laptime =**838.6 s** totalconsumption =**1.8006 kWh** w1mean =**6.7698 km/h** w2mean =**7.1112 km/h** w3mean =**7.5334 km/h**
a	M=310 kg powcoeff=max(min(3,0.5*(9.072-v(i))),0)/3	laptime = **838.6 s** totalconsumption = 1.7513 kWh
b	M=350 kg powcoeff=max(min(3,0.5*(9.20-v(i))),0)/3	laptime = **838.6 s** totalconsumption = 1.8491 kWh
c	M=310 kg powcoeff=max(min(3,0.5*(9.37-v(i))),0)/3	totalconsumption = **1.8002 kWh** laptime = 820.8 s 17.8 s gain
d	M=350 kg powcoeff=max(min(3,0.5*(8.89-v(i))),0)/3	totalconsumption = **1.8004 kWh** laptime = 858.6 s 20.0 s loss
e	Power=2.5 kW powcoeff=max(min(3,0.5*(8.66-v(i))),0)/3	totalconsumption = **1.8011 kWh** laptime = 825.0 s 13.6 s gain
f	Power=2.5 kW, M=340 powcoeff=max(min(3,0.5*(8.55-v(i))),0)/3	totalconsumption = **1.7996 kWh** laptime = 833.6 s 5.0 s gain
g	No slopes powcoeff=max(min(3,0.5*(11.48-v(i))),0)/3	totalconsumption = **1.8004 kWh** laptime = 683.6 s 155 s gain
h	Faster in curves, fcorsafe=0.7 powcoeff=max(min(3,0.5*(11.58-v(i))),0)/3	totalconsumption = **1.8018 kWh** laptime = 669.000 s 169.6 s gain

i	Alternating speed totalconsumption = 1.65/2 in 1st half totalconsumption = 1.95/2 in 2nd half	laptime1 = 922.800 s laptime2 = 786.000 s 31.6 s loss

As stated in Section 5.2 the total energy for the race is calculated as 1800 kWh. The other parameters are selected in the possible range for a solar car. They are selected close to Hasat's values but with the lack of some measurements the set of values can not be said to be its values. But it is important here that, a car having these specifications will perform as predicted by the program.

Case a: The energy required in the case of decreasing the mass of the car by 20 kg and keeping the lap time constant is calculated. It is seen that total consumption comes down to 1.751 kWh. In other words, 6.06% decrease in weight leads to 2.71% decrease in total energy consumption.

Case b: The energy required in the case of increasing the mass of the car by 20 kg and keeping the lap time constant is calculated. It is seen that total consumption goes up to 1.849 kWh. In other words, 6.06% increase in weight leads to 2.73% increase in total energy consumption.

The cases "a" and "b" display the sensitivity of energy consumption to total mass keeping the lap time constant. Since the energy available for the race is assumed to be constant the following cases keep the energy constant and display the sensitivity of lap time on the changes.

Case c: The effect of decreasing mass by 20 kg corresponds to gaining 17.8 s in one lap. (6.06% decrease in mass, 2.12% decrease in lap time)

Case d: The effect of increasing mass by 20 kg corresponds to losing 20.0 s in one lap. (6.06% increase in mass, 2.39% increase in lap time)

Case e: Increasing the peak power value from 2.0 kW to 2.5 kW brings 13.6 s of advantage in one lap. (1.62% gain in lap time)

It is seen in case “e” that increasing the power is advantageous but if a more powerful motor also adds some weight. Keeping in mind that, it is the lap time to be improved the effect of selecting that motor must be known. This is given in case “f”

Case f: If the team selects the 10 kg heavier 2.5 kW motor, the lap time decreases by 5 s. Therefore the more powerful motor turns out to be a better choice even though it is 10 kg heavier.

Increase in peak power improves the performance because it keeps the speed higher in uphill gradients while going slower on level road. Therefore the weighted average speeds converge to the average speed. In other words the speed distribution data graph has more of its points close to the average speed. But if the battery characteristics are integrated into the program then the increase in peak power will bring decrease in battery efficiency therefore this will decrease the available power during the race.

Case g: In Section 1.3, it is described that the track has steep gradients making the race demanding. How the same car would perform on a track with the same top view but all level in side view is given in this case. The result is a gain of 155 s.

Case h: The advantage of taking the curves faster is shown in this case. The factor of cornering safety is defined as the ratio of allowed speed to the speed of taking that curve with 1 g lateral acceleration. In this case this factor is changed from 0.5 to 0.7. The resulting effect is 169.6 s of gain.

Case i: The car consumes less energy than available in the first half (1.65kWh

instead of 1.8 kWh) due to an error in the driving input. The input is corrected for the second half considering the remaining energy available (1.95 kWh). The race is completed with this adjustment. The energy consumption is the same but the time lost because of this error is 31.6 seconds in every two laps.

CHAPTER 6

CONCLUSION

The intended purpose of this study is to guide a beginner in solar race car design in some important aspects. These aspects are the design of the body, the aerodynamics analyses that need to be conducted on the body, the usage of the results in the dynamics calculations and predicting the race performance. The results of performance predictions supplies valuable data for the previous steps. In fact, these steps may need to be repeated several times. The other aspects of the design, such as the 3D modeling and strength design of the chassis, the brake system, and the suspension system are all handled by another team member, who played an important role in production also. On the electrical side, acquisition of the motor, its driver, the batteries, the solar panels, integration of the panels onto the body and long and time consuming cabling are also carried out by other team members. Since this thesis includes one year of design and production experience and very useful basic tools which will always be required, it can be repeatedly used and referred in the following years.

Although design is an infinite, iterative process, some facts, such as finite time and money require truncation of the continuous improvement phase.

In ideal case, first the decision of number of wheels is done. Assuming that the three-wheeled configuration is selected, after using the tools for determining the location of the center of gravity, either an optimal or a satisfactory solution is obtained. To be able to do this, the tires must be selected and experiments must be conducted to get the dry friction coefficient between the tire and the asphalt. Then, within the limits of rules given in FIA Handbook, the chassis, the roll bar and the

cover are designed considering the aerodynamic concerns mentioned in Chapter 3. It is possible to design a monocoque chassis to replace the chassis and cover, if possible within the production abilities.

The preliminary design is placed on the virtual circuit and the telemetry data is collected from the race simulation. This data is useful in both aerodynamic design and the race strategy. The race strategy can be thought of as a long list of instructions to complete the race with the best possible performance. These instructions may include position, velocity, acceleration and steering angle input at any time in the race. Using the weighted averages the speed at which most of the energy is dissipated is found and the aerodynamic design is revised and optimized for this speed.

In practice however, within a short period of time and with little manpower the procedure had to be a single shot solution. The chassis had to be produced before purchasing the tires and the motor. The motor that shipped was different from the motor purchased and was not able to perform as intended.

After the production of the car, everything is fixed but, the driving characteristics remain as a variable. As stated in Chapter 4, the most important part is to know at what speed the race will be run the most efficiently. To know this, of course, several races must be completed and telemetry data must be compared in virtual or real race tracks. After estimating the average speed, the effort goes to maintaining constant a speed wherever possible. Since the race is on a Formula 1 track with gradients and tight curves the racing strategy is not as straightforward as in the highway races being held in the world.

REFERENCES

[1] *WSC,* 2006, History of World Solar Challenge, World Solar Challenge Organization, viewed 22 November 2006.
http://www.wsc.org.au/history/

[2] *American Solar Challenge,* 2006, About the Rayce, North American Solar Challenge, viewed 22 November 2006.
http://www.americansolarchallenge.org/

[3] *Racing Cars Powered by Solar Energy!,* 2006, Solar Racing Cars & Races, EcoBusinessLinks Ltd., viewed 22 November 2006
http://www.ecobusinesslinks.com/solar_cars_solar_races.htm

[4] *FIA,* 2004, "Technical Regulations for Electro-Solar and Alternative Energies Vehicles"
http://www.fia.com/

[5] A*urora Solar Car,* 2006, Aurora's 2005/06 Program, Aurora Vehicle Association Inc., viewed 22 November 2006
http://www.aurorasolarcar.com/main_frame.html

[6] Dresselhaus M. S., Thomas I. L., 2001, "Alternative Energy Technologies," Nature, **414**, pp. 332-337.

[7] Laherrere, J., "Estimates of Oil Reserves" Paper presented at the EMF/IEA/IEW meeting IIASA, Laxenburg, Austria, June 19, 2001.

[8] Vitousek P. M., 1994, "Beyond Global Warming: Ecology and Global Change," Ecology, **75**, pp. 1861-1876.

[9] Solar Energy Irradiation Data supplied to the Formula-G Solar Car teams by Tubitak, on July 1, 2005.

[10] Green, M. A., Emery, K., King, D. L., Hisikawa Y. and Warta, W., 2006, "Solar Cell Efficiency Tables (Version 27)," Prog. Photovolt, Res. Appl., **14**, pp. 4551.

[11] Sonntag, R. E., Borgnakke, C., Van Wylen, G. J., 1998, Fundamentals of Thermodynamics, 5/e, Wiley & Sons, Inc., NY, US, pp. 542.

[12] Arsie, I., Marotta, M., Pianese, C., Rizzo, G., Sorrentino M., 2003, "Optimal Design of a Hybrid Electric Car with Solar Cells," 1st AUTOCOM Workshop on Preventive and Active Safety Systems for Road Vehicles.

[13] Goyal, A., Khalaf, R., Mehta, A., Somani, A., Somani, P., 2000, "Solar Eclipse: The Failure of a Promising Technology," The Structure of Engineering Revolutions.
http://web.mit.edu/6.933/www/Fall2000/solarEclipse.pdf

[14] Singh, P., Glahn, P., Koffke, W., 1991, "The Design and Construction of a Solar Electric Commuter Car," IEEE Photovoltaic Specialists Conference Records, **1**, pp.712-716.

[15] Shimizu, Y., Komatsu Y., Torii, M., Takamuro, M., 1998 "Solar Car Cruising Strategy and Its Supporting System," JSAE Review, **19**, pp. 143-149.

[16] Trapp, J., Zores, R., *NACA 4 Digits Series* 2006, NACA 4 Digits Series,

viewed 22 November 2006.
http://www.pagendarm.de/trapp/programming/java/profiles/NACA4.html

[17] Örselli, E., 2006, "Computation of Drag Force on Single and Close-Following Vehicles," MS. Thesis, Middle East Technical University, Ankara, Turkey.

[18] Daniels, M. W., and Kumar, P. R., 1997, "Racing with the Sun: The Optimal Use of the Solar Power Automobile," Proceedings of the 36th Conference on Decision & Control San Diego, California USA, pp. 571-576.

[19] Howlett, P., Pudney, P., Tarnopolskaya, T., Gates, D., 1997, "Optimal Driving Strategy for a Solar Car on a Level Road," IMA Journal of Mathematics Applied in Business & Industry, **8**, pp. 59-81.

[20] Santosa, F., 2001, "Solar Car Racing Strategies,"
http://www.sfu.ca/~qlib/publications/solar.pdf

[21] Pudney, P., Howlett, P., 2002, "Critical Speed Control of a Solar Car," Optimization and Engineering, **3**, pp. 97-107.

[22] Wright, G. S., 1996, "Optimal Energy Management for Solar Car Race," IEEE 39th Midwest symposium on Circuits and Systems, **3**, pp. 1011-1014.

[23] Kennedy, B., Patterson, D., Camilleri S., 2000, "Use of lithium-ion batteries in electric vehicles," Journal of Power Sources, **90**, 156-162.

APPENDIX A

DYNAMICS08.M MATLAB PROGRAM

Table A.1 `Dynamics08.m`

Input:	
xdata=[0000 0250 0540 1040 1400 1530 1930 2380 2570 2760 3180 3410 3690 4010 4470 4780 5070 5377];	distance of start of each interval from the beginning [m]
sdata=[0.00000 -0.06475 0.06944 -0.07495 -0.01205 -0.04326 0.07481 -0.02150 0.01622 -0.08145 -0.01453 0.07030 -0.01843 0.06730 -0.02423 0.01190 0.00000];	
energy=0;	
laptime=0;	
M=330;	[kg]
dt=0.2;	[s]
afr=0.5*1.225*1*0.34;	0.5 * ρ_{air} * A_{cs} * $C_{d,tot}$ [kg/m]
bfr=1;	[kg/s]
cfr=10; %	[kg m/s/s]
apower=-0.0003487;	
bpower=0.235;	
cpower=80;	
theta=-3*pi/180	
t=0;	[s]
wf=0.25*M*9.81;	[N]
i=1;	
mu=0.5;	coefficient of friction [ ]
x=0;	position [m]
v=0.01; % [m/s]	initial speed [m/s]
w= zeros(25)	

Calculations:	

for lap=1:3
  for interval=1:17
  slope=sdata(interval);
  theta=asin(slope);
  energy;
  ft1max=wf*cos(theta)*mu;
	maximum tractive force limited by power [N]

% maximum tractive effort limited by friction [N]
  while xdata(interval)<=x(i) & x(i)<xdata(interval+1)
  power(i)=max(min(3,0.5*(12-v(i))),0)*(apower*v(i)*v(i)*v(i)+bpower*v(i)*v(i)+cpower*v(i));
denergy(i)=power(i)*dt;
  energy(i+1)=energy(i)+denergy(i);
  fr(i)=afr*v(i)*v(i)+bfr*v(i)+cfr+M*9.81*slope;
  ft2max(i)=power(i)/v(i); %
	power output [W]
	resistant force [N]
	maximum tractive force limited by power [N]

ft(i)=min(ft1max,ft2max(i));
  fn(i)=ft(i)-fr(i);
  a(i)=fn(i)/M;
  dv(i)=a(i)*dt;
  v(i+1)=v(i)+dv(i);
  dx(i)=v(i)*dt;
  x(i+1)=x(i)+dx(i);
  t(i+1)=t(i)+dt;
  slop(i)=slope;
  w(ceil(v(i)))=w(ceil(v(i)))+1;
  if x(i)>404 & x(i)<533.1
  figure(7);hold on;plot(x(i),14,'r');
  end
  if x(i)>554 & x(i)<=720
  figure(7);plot(x(i),17,'r');
  end
  if x(i)>1109 & x(i)<=1271
  figure(7);plot(x(i),15,'r');
  end
  if x(i)>1271 & x(i)<=1540
  figure(7);plot(x(i),14,'r');
  end
  if x(i)>2007 & x(i)<=2156
  figure(7);plot(x(i),14,'r');
  end
	tractive effort [N]
	net force [N]
	acceleration [m/s/s]

```
        if x(i)>3407 & x(i)<=3523
            figure(7);plot(x(i),14,'r');
        end
        if x(i)>4785 & x(i)<=5081
            figure(7);plot(x(i),14,'r');
        end
        i=i+1;
      end
   end
   if x(i)>=5377
      vmean=lap*5377/t(i)
      x(i)=0;
      laptime(lap+1)=t(i)-sum(laptime)
      lap
      energy;
   end
end
power(i)=power(i-1);slop(i)=slop(i-1);
energy;
vmean=x(i-1)/t(i-1);
for vel=1:25
   w1(vel)=w(vel)*vel^1;
   w2(vel)=w(vel)*vel^2;
   w3(vel)=w(vel)*vel^3;
end
wmean=w/sum(1:25);
w1mean=sum(w1)/sum(w)
w2mean=(sum(w2)/sum(w))^(1/2)
w3mean=(sum(w3)/sum(w))^(1/3)
w=w/sum(w);
w1=w1/sum(w1);
w2=w2/sum(w2);
w3=w3/sum(w3);
```

Displaying the results:

```
vscale=1;
ascale=10;
sscale=10000;
%figure(1);
hold on;
plot (t,x,'k-');
plot(t,slop*sscale,'-');
```

```
ylabel('distance [m]');
xlabel('time [s]');
legend('distance','slope x10000',-1);
text(50,300,'string');
%figure(2);
hold on;
plot(t,power,'k-');
plot(t,slop*sscale,'-');
plot(t,energy/100,'r-');
xlabel('time [s]');
legend('power [W]','slope x10000' ,'energy [J]',0);
%plot(t,fn,'g');
text(50,300,'string');
%figure(3);
hold on;
plot (t,v*vscale,'k-');
plot(t,slop*sscale/100,'-');
ylabel('velocity [m/s]');
xlabel('time [s]');
text(50,300,'string');
%legend('v',-1);
% plot(t,a*ascale,'r');
%figure(4);
hold on;
plot(t,v,t,power/1000);
xlabel('time [s]');
legend('speed [m/s]','power [kW]',0);
%figure(5);
hold on;
plot(t,slop*10,t,power/1000);
xlabel('time [s]');
legend('slope x10 [ ]','power [kW]',0);
%figure(6);
hold on;
plot(w,'k');
plot(w1,'r-.');
plot(w2,'g');
plot(w3,'b');
figure(7);
hold on;
plot(x,v,'b');
xlabel('position [m]');
```

APPENDIX B

FIGURES FROM THE CAR MODEL AND STRUCTURAL ANALYSES

The following figures are provided by the team designer Orçun Yıldırım.

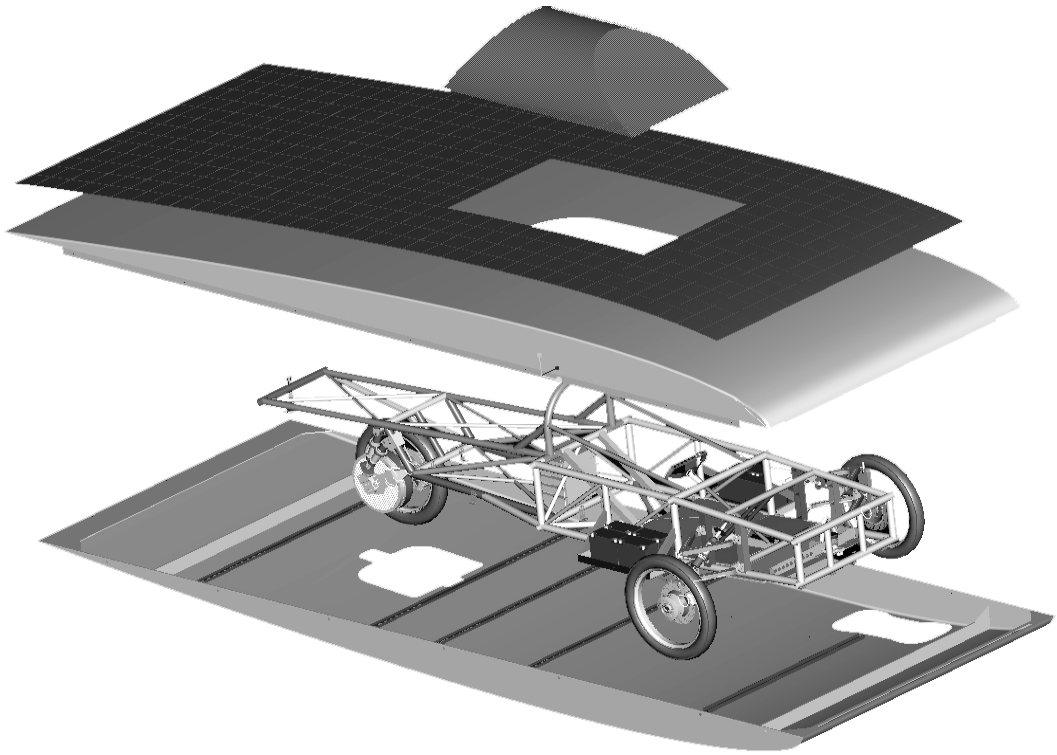

Figure B.1 Exploded view of the car assembly

In this figure, from top to bottom, the canopy, solar panels, the top half of the shell body and at the bottom, the bottom of the shell body are shown separate from the remaining. The remaining consists of the chassis, the suspension system, the steering system, the electric motor, its driver and the batteries.

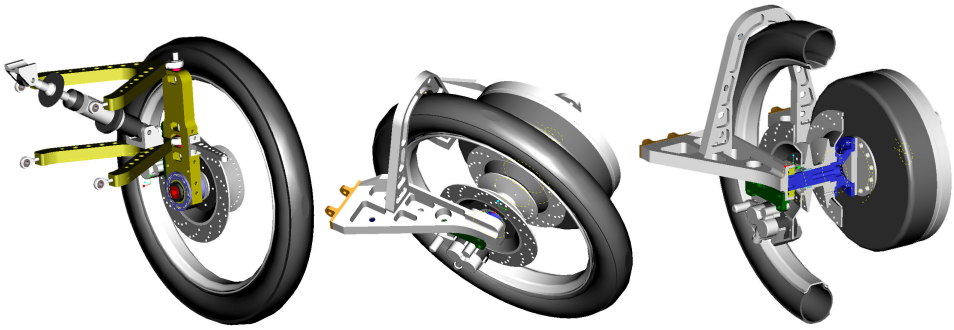

Figure B.2 Suspension system parts
left: front suspension, middle: rear suspension, right: rear suspension, section view

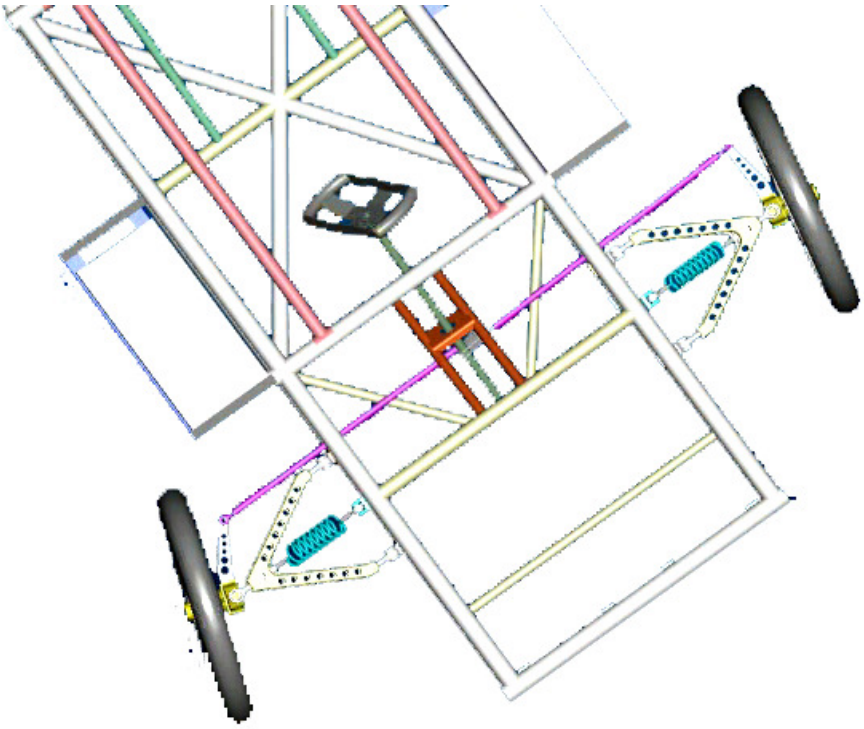

Figure B.3 Front wheels and steering system, top view

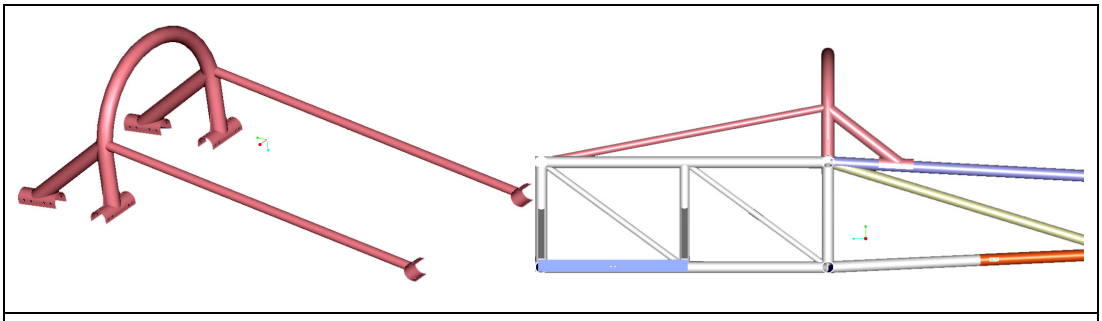

Figure B.4 left: roll bar, right: its position on the chassis

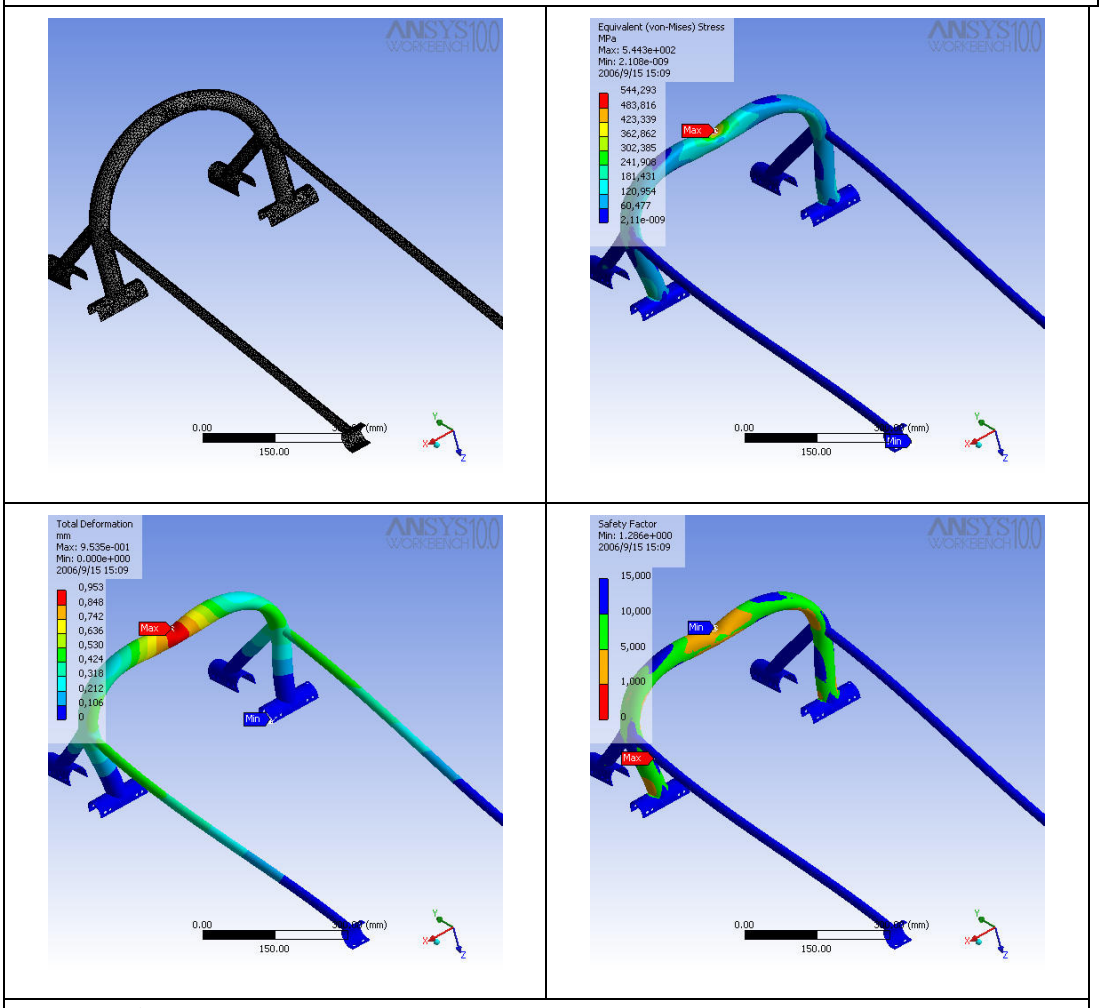

Figure B.5 Figures that belong to analyses of force acting from top
left top: mesh structure
right top: contours of equivalent stress
left bottom: contours of total deformation
right bottom: contours of safety factor

Analysis on load carrying capacity of the roll bar from top according to the rules

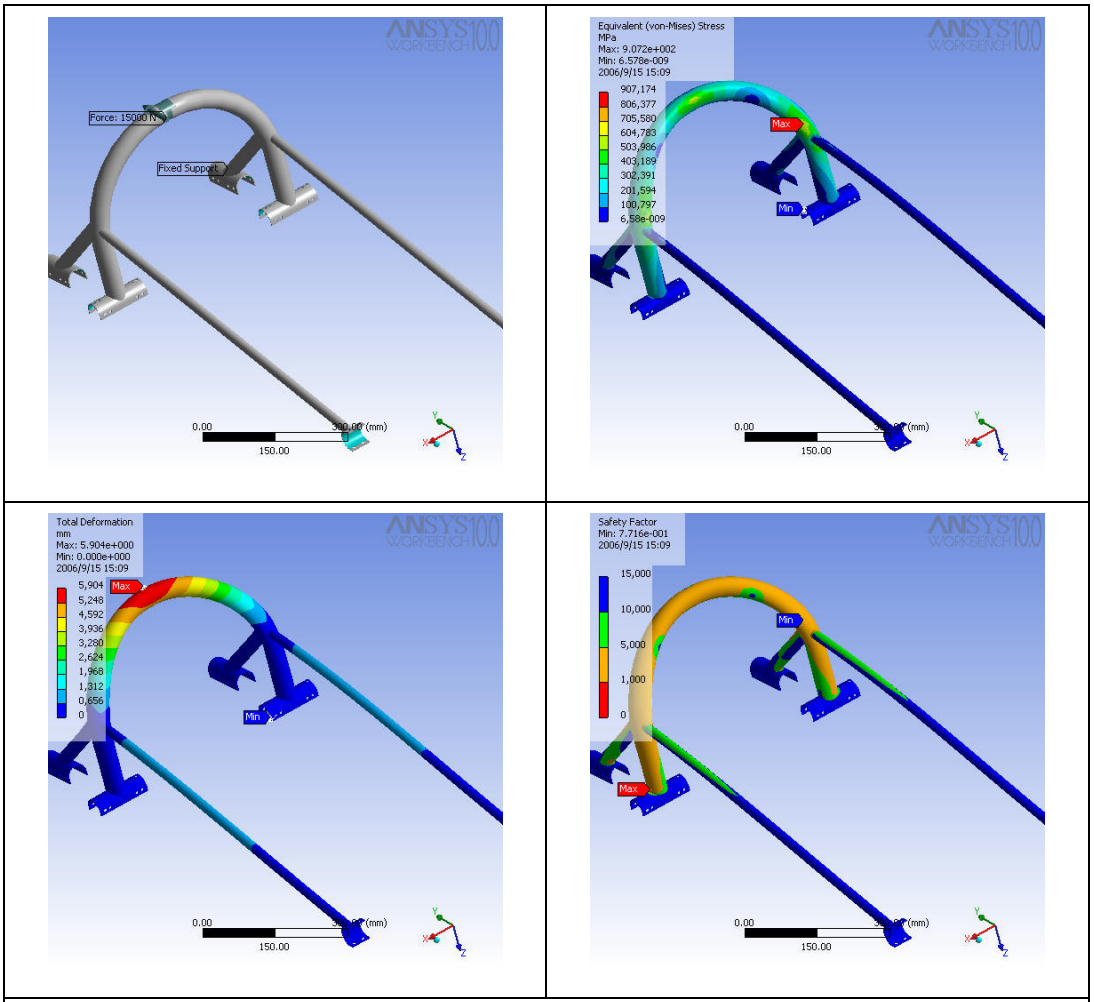

Figure B.6 Figures that belong to analyses of force acting from front
left top: mesh structure
right top: contours of equivalent stress
left bottom: contours of total deformation
right bottom: contours of safety factor

Analysis on load carrying capacity of the roll bar from front according to the rules